

CHAPTER 5

Results and discussion (part II):

Materials characterization of potassium sodium niobate based silicate glass and glass-ceramics

In this chapter, materials characterization of transparent glass-ceramics containing ferroelectric potassium sodium niobate ($(K_{0.5}Na_{0.5})NbO_3$ (KNN) crystals in a silicate (SiO_2) glass system were studied. In this topic, the incorporation method was used in glass preparation process like chapter 4. The well prepared glasses were subjected to heat treatment in order to growth the crystals inside glass matrix. The basic properties like physical, electrical, optical and microstructure have been carried out in this chapter. In first section, the properties of 75KNN-25 SiO_2 and 80KNN-20 SiO_2 have been demonstrated. After that, in the next section, the suitable glass was selected to dope with Er_2O_3 in order to study the effect of doping Er_2O_3 to glass properties, especially optical property. The study ensured that Er_2O_3 dopant had a lot effect to glass-ceramics which will mention later in section 5.2.

5.1 The characterization of KNN- SiO_2 glass and glass-ceramics

The single phase KNN was first mixed with silica in composition ratio of 75KNN-25 SiO_2 , refers to our previous work [14,119]. We have reported that the transparent glass-ceramics KNN was found in glass-ceramics with percent of silica are lower than 30%. The glass-ceramics with 25mol% of silica showed high stability and dielectric constant. Thus, the aim in this study is to find out which percentages of silica that optimizes for crystallization process. We are varied silica in range of 25mol% and 20mol%. The weight percent of 75KNN-25 SiO_2 and 80KNN-20 SiO_2 glasses are already calculated and showed in Table 3.3 in chapter 3.

Thus, in this work, the prepared KNN powder was mixed with SiO_2 in a composition of 75:25 mol% and 80:20 mol% and melted at 1300°C for 15 min. Then melted glass was

then quenched at room temperature (about 30°C). The quenched glasses were subjected to heat treatment schedules in order to study the effect of subsequent heat treatment temperature on phase formation. To analyze the glass and glass-ceramic properties, various techniques were employed. XRD and SEM techniques were used to investigate the phase composition and to observe the microstructure of the glass and glass-ceramic samples. The room temperature dielectric constant (ϵ_r) and dielectric loss ($\tan\delta$) of the glass-ceramics measured at various frequencies and temperature were used to study the electrical property. Finally, the transmission and refractive index values were measured for investigated the optical property.

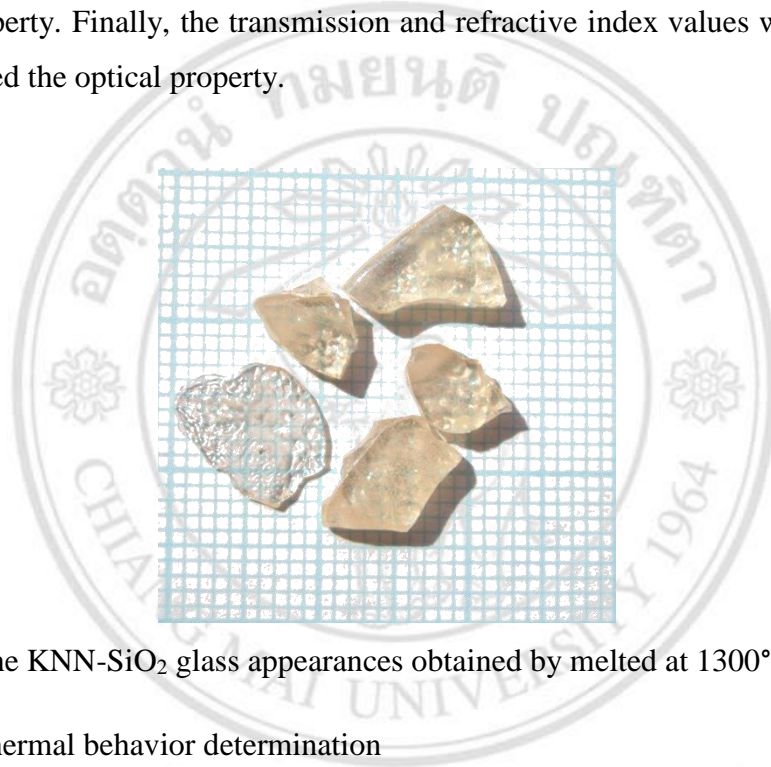


Figure 5.1 The KNN-SiO₂ glass appearances obtained by melted at 1300°C for 15 min.

5.1.1 Thermal behavior determination

The example of as-quenched glasses appearance was showed in Fig. 5.1. Sample glasses from two conditions (75KNN-25SiO₂ and 80KNN-20SiO₂) are all transparent and light yellowish as showed in Fig. 5.1. The DTA traces of the 75:25 mol% and 80:20 mol% KNN glasses are shown in Fig. 5.2. The endothermic peaks and exothermic peaks correspond to the glass transition (T_c) and crystallization temperature (T_g). The glass thermal stability factor ($\Delta T = T_x - T_g$; Hrubby's criterion [120]) was found to be approximately 85°C for the 75KNN-25SiO₂ and 80°C for the 8KNN0-20SiO₂ system, meaning that the 80:20 mol% glass has slightly lower stability than that of 75:25 mol% glass. The high thermal stability factor specifies the ability of glass to form

nano-structured glass–ceramics that controlled heat-treatment. The two glass systems were then subjected to heat treatment schedules depending on their T_g and T_c . The glass appearance is shown in Fig. 5.3.

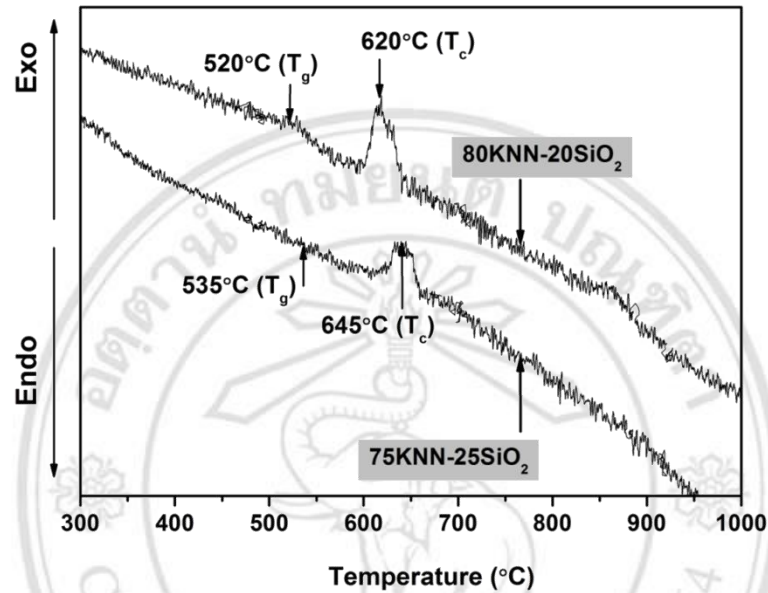


Figure 5.2 DTA traces of the as-quenched glasses from 2 glass series.

Table 5.1 The thermal profile and glass stability factor of 75KNN-25SiO₂ and 80KNN-20SiO₂ glasses. (T_g = Glass transition temperature, $T_x = T_c$ onset point, T_c = Crystallization temperature, ΔT = Glass stability)

Glass conditions	T_g	T_x	T_c	ΔT
75KNN-25SiO ₂	535	620	645	85
80KNN-20SiO ₂	520	600	620	80

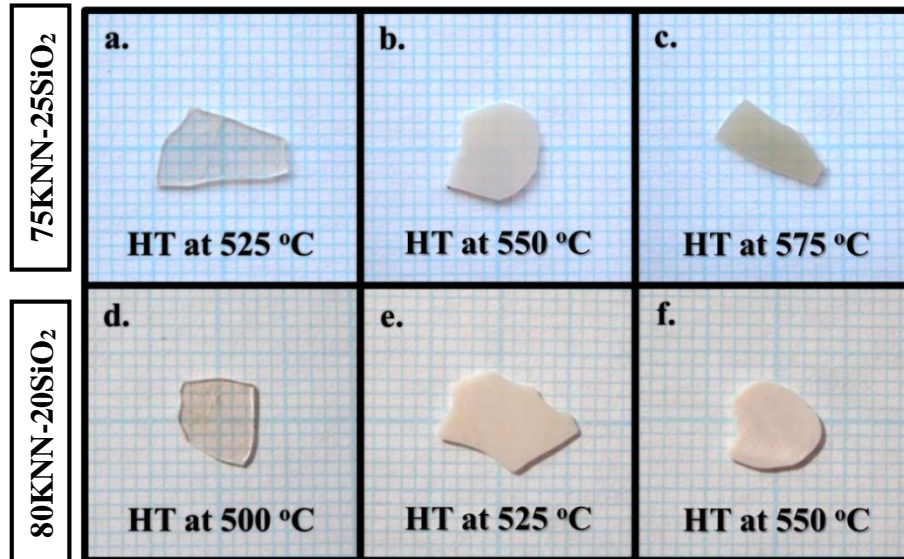


Figure 5.3 The appearance of glass-ceramics from 2 glass series with different heat treatment temperature (**a.-c.** 75KNN-25SiO₂ and **d.-f.** 80KNN-20SiO₂)

5.1.2 Densification investigation

From Fig. 5.4, the density of the as-quenched glass was the lowest, and the heat treatment caused a general increase in density, as well as their dielectric constant (ϵ_r). It can be assumed that the higher density and ϵ_r of these glass ceramics resulted from the growth of the KNN crystals during the crystallization process.

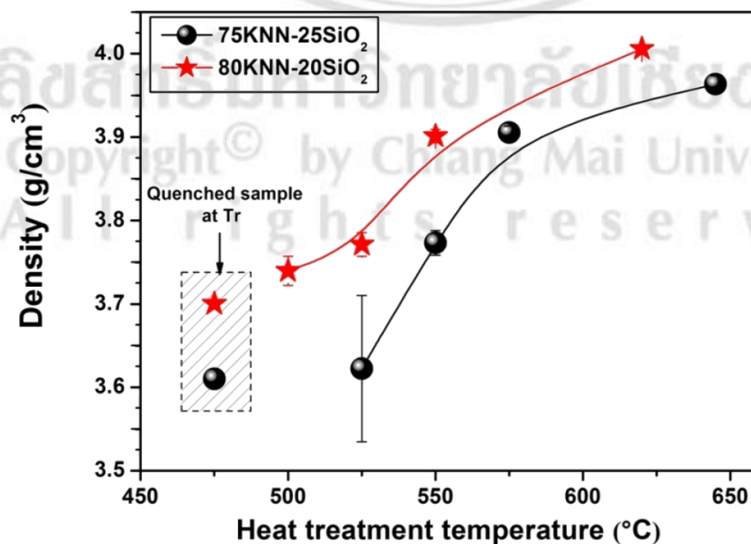


Figure 5.4 The density of 2 glass series varied with heat treatment temperature.

5.1.3 Structural formation

1) Phase composition studied by XRD

The XRD patterns in Fig. 5.5 show diffraction peaks of the as-quenched glass and glass-ceramics. In both the 75KNN-25SiO₂ and 80KNN-20SiO₂ systems, the XRD patterns of the as-quenched glass and heat treated glass at 525°C and 500°C contain only a broad peak around the diffraction angle of $2\theta = 30$, which indicates a highly amorphous nature. The samples heat treated at higher temperatures (75KNN-25SiO₂; HT > 525°C, 80KNN-20SiO₂; HT > 500°C) have diffraction peaks around $2\theta = 23^\circ, 32^\circ, 46^\circ, 52^\circ$ and 57° , which confirms the existence of crystalline phases in the amorphous matrix. These crystalline phases were assigned to the potassium sodium niobate crystal phase (JCPDS number 77-0038). However, in the 80KNN-20SiO₂ glass system, other additional diffraction peaks occurred, which were marked as unidentified phases (*).

The calculated average crystallite sizes are summarized in Table 5.2. It can be seen that the crystallite size analyzed from XRD were increased with increasing heat treatment temperature. The full width at half maximum (FWHM) values of the intense diffraction peak detected from XRD patterns, the average crystallite sizes (diameter, d) were calculated by conventional procedure using the Scherrer's equation [97] (equation 4.3).

2) Phase formation studied by Raman spectroscopy

The raman spectra of KNN-SiO₂ from Fig. 5.6 showed the a little bit different between 2 glass series. All heat treated glass-ceramics exhibit 3 main scattering peaks at around 235 cm⁻¹(ν_5), 600 cm⁻¹(ν_1) and 880 cm⁻¹($\nu_1 + \nu_5$). This strong peak at 246 cm⁻¹ and 604 cm⁻¹ and weak peak at 880 cm⁻¹ indicates typical perovskite structure of KNN in glass-ceramics [121].

Normally, KNN has orthorombic $Amm2 - C_{2v}^{14}$ space group, yields raman active optical modes of $4A_1+4B_1+3B_2+A_2$ which is consisting

translational modes of cations and internal modes of NbO₆ octahedral [122]. A₂ represent of IR active mode, thus KNN have total 12 Raman active modes and 11 IR active modes. The NbO₆ octahedron exhibits cubic Oh symmetry and consists of six normal vibrations [56,123].

$$\Gamma_{\text{vib.}} = 1A_{1g}(v_1) + 1E_g(v_2) + 2F_{1u}(v_3, v_4) + F_{2g}(v_5) + F_{2u}(v_6) \quad (2)$$

Among the vibration modes of octahedra, A_{1g}(v₁), E_g(v₂) and F_{1u}(v₃) are the stretching mode, whereas F_{1u}(v₄), F_{2g}(v₅) and F_{2u}(v₆) are the bending mode. It has been shown that a substitution of A-site ions with a smaller (lighter) ion will shorten the distance between Nb⁵⁺ and its coordinated oxygen atoms, causing an increase in the binding strength and then a shift of the v₁ stretching mode to higher frequencies [56].

The glass with the same K₂O/Nb₂O₅ also increased the raman intensity with SiO₂ content [124]. As can see from Fig. 5.6, glass with 30 mol% of SiO₂ showed higher intensity than 20 mol% SiO₂ contained. However, heat treatment is the significant role to changing the raman intensity. After heat up to 650°C, the raman peaks changed to higher intensity and the main strong peak had a bit shifted because of the formation of crystal phase in amorphous matrix and the distorted of its crystal structure.

Recently, many works have been focused on how K⁺, Na⁺ and Nb⁵⁺ bonded with based glass like silicate. They state that Nb-O vibration mode is the huge respond in raman spectrum. The increasing intensity of peak around 850-900 cm⁻¹ is relate to the vibration of highly distortion NbO₆ octahedra. Lipovskii et al. [125] had reported that the high intensity of raman peak around 850 cm⁻¹ is become of the replacement of sodium with potassium in glass composition. However, the raman spectra in range of 870-950cm⁻¹ is also corresponded to the vibration of Nb-O non-bridging bond. Alekseeva et al. [126] have reported that Raman spectrum of the 25K₂O-27.5Nb₂O₅-47.5SiO₂ glasses show highest band around 800–950 cm⁻¹, in which related to the vibration of NbO₄ tetahedra. Therefore, Guo et al. [127] have reported the EXAFAS spectroscopy studied in niobosilicate glasses. They found that glass

with low contents of Nb_2O_5 ($\text{Nb}_2\text{O}_5 \leq 15\text{mol}\%$ and $\text{SiO}_2 \geq 57.6\text{ mol}\%$) showed the raman spectra band at $870\text{-}910\text{ cm}^{-1}$ which are related to the vibration of highly distorted NbO_6 octahedra or the NbO_6 octahedral having at least a short terminal Nb-O bond pointing towards a modifier ion [128-129].

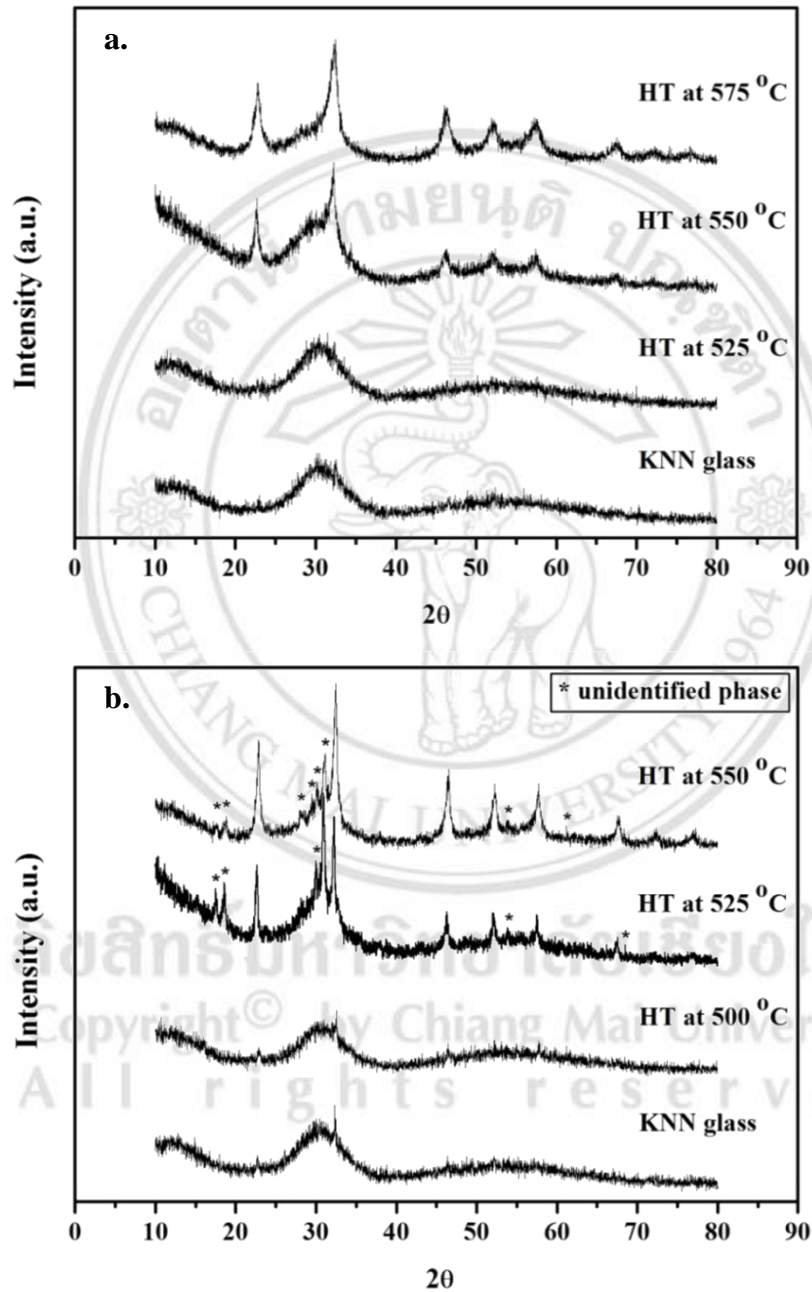


Figure 5.5 XRD patterns of glass-ceramic samples at various temperatures.

a) 75KNN-25SiO₂ system, b) 80KNN-20SiO₂ system.

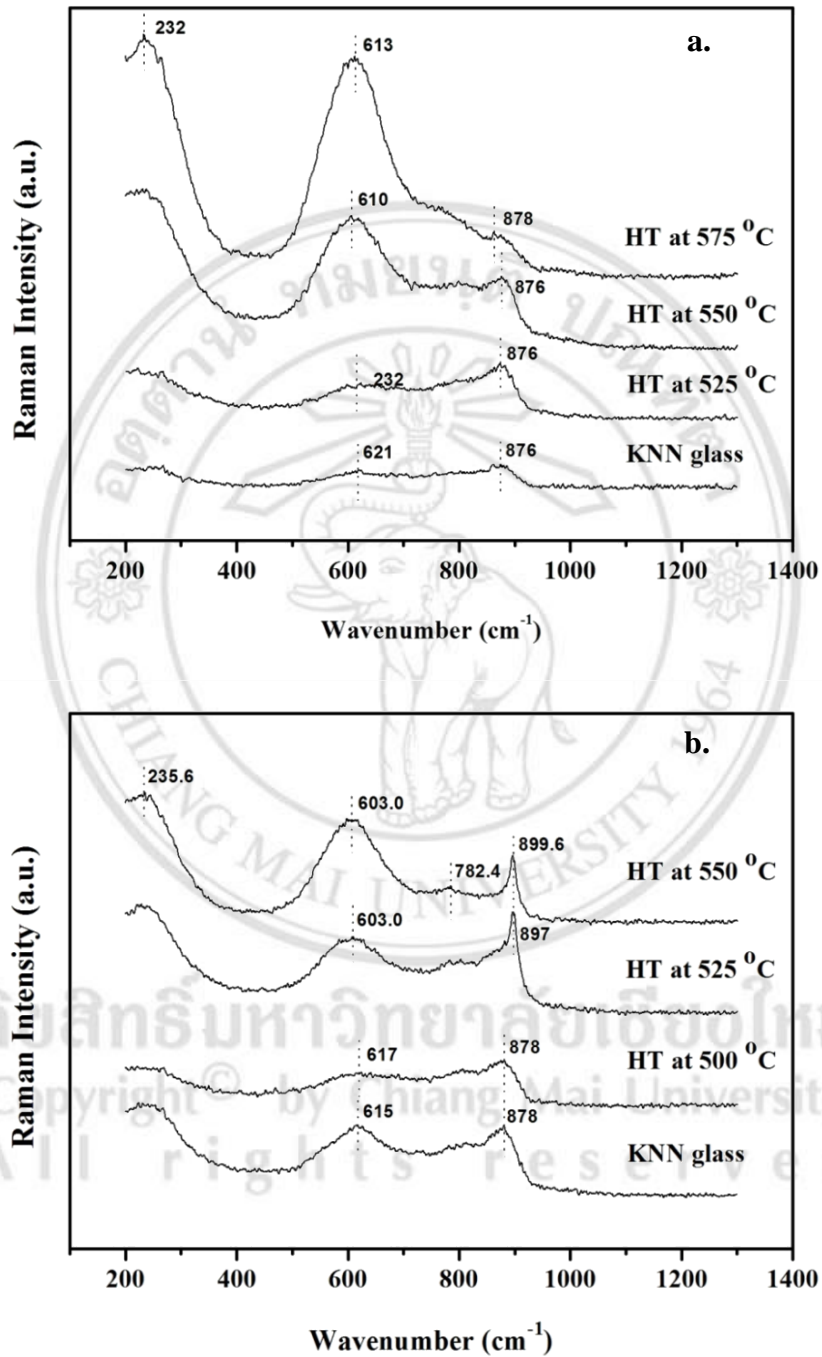


Figure 5.6 Raman spectra of glass-ceramic samples at various temperatures.

a) 75KNN-25SiO₂ system, **b)** 80KNN-20SiO₂ system

5.1.4 Microstructural observation

The morphology and crystallite size in glass–ceramic samples have been investigated by FE-SEM image analysis as shown in Fig. 5.7. The SEM micrographs show a bulk crystallization of the KNN phase with a rectangular shape occurring in the glass matrices of a lowest heat treatment samples for both 75KNN-25SiO₂ and 80KNN-20SiO₂, but in the higher heat treatment samples the irregular shape of crystals are revealed. The increments in the size of crystals embedded in the glass matrix caused degradation with the glass transparency due to light scattering from the glass sample that has a crystallite size larger than 200 nm. The crystals of all samples are homogeneously embedded throughout the glass matrix with random orientations. The average crystal sizes were observed from the SEM micrographs and summarized in Table 5.2, showing the diagonal values (*D*) and length values (*L*) of the crystals in both 75KNN-25SiO₂ and 80KNN-20SiO₂ glass ceramics comparing with crystallite size which calculated from Scherrer's equation. The EDS analysis from SEM micrograph was illustrated in Fig. 5.8.

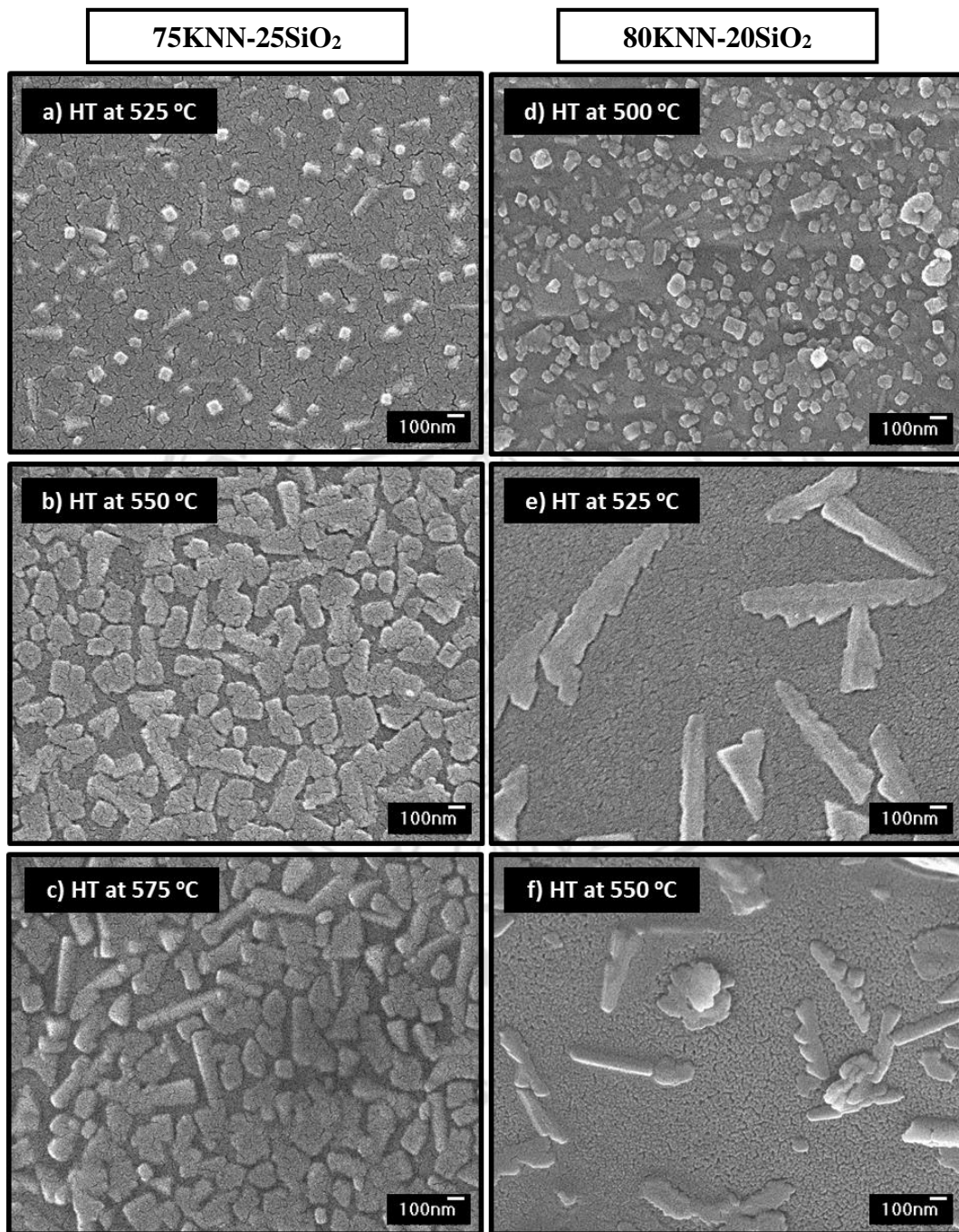


Figure 5.7 SEM micrographs of glass-ceramic samples after heat treatment at various temperatures.

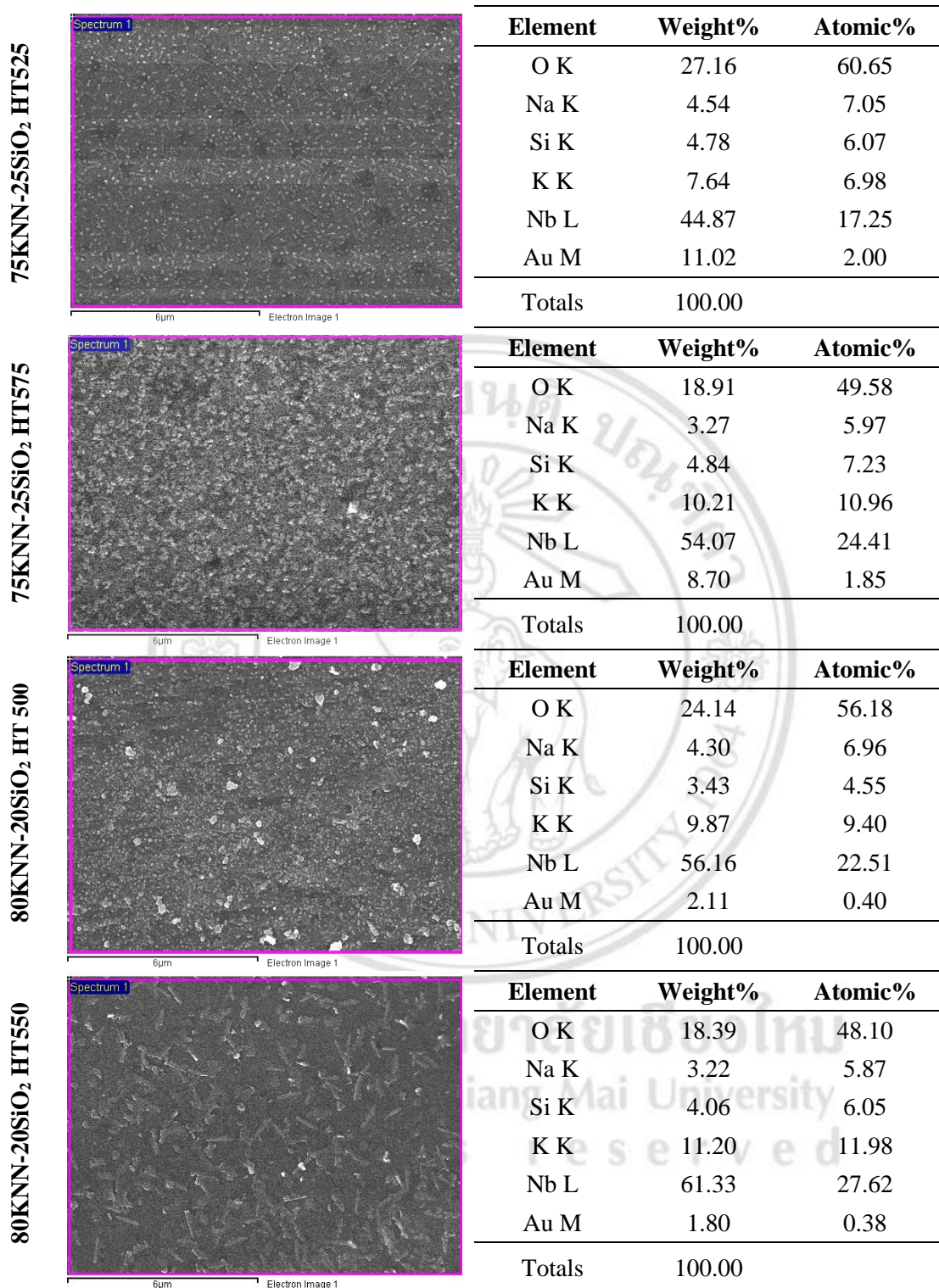


Figure 5.8 EDS analysis from SEM micrograph of glass-ceramics 75KNN-25SiO₂ and 80KNN-20SiO₂ which heat treatment at different temperatures.

Table 5.2 Physical properties data of 75KNN-25SiO₂ and 80KNN-20SiO₂ glass systems. (**L*, length, *D*, diagonal values, *d*, crystallite size)

Heat treatment temperature (°C)	Density (g/cm ³)	Average crystallite size (nm)		
		SEM micrograph		XRD analysis
		<i>L</i>	<i>D</i>	<i>d</i>
75 KNN – 25 SiO₂				
As- quenched glass	3.61	-	-	3.2837
525	3.62	219.30±16	108.94±3	6.5385
550	3.77	294.74±22	188.82±15	35.005
575	3.91	444.24±35	266.45±18	21.0161
80 KNN – 20 SiO₂				
As- quenched glass	3.70	-	-	35.0215
500	3.74	116.45±10	109.32±8	35.0319
525	3.77	886.84±57	157.23±10	41.8849
550	3.90	478.38±31	175.75±27	35.0289

It can be seen from Table 5.2 that the crystallite size of from both 75KNN-25SiO₂ and 80KNN-20SiO₂ increased with an increasing heat treatment temperature. At the lowest heat treatment temperature, the crystallite size was smaller than 200 nm and may give less light scattering than the larger crystals. The SEM micrographs of the 80KNN-20SiO₂ glass-ceramic samples heated at 525°C and 550°C show a different morphology than other samples. This may be due to the occurrence of secondary phases as confirmed by XRD results shown in Fig. 5.5.

5.1.5 Electrical property

In Fig. 5.9, the relationship of the dielectric constant (ϵ_r) and dielectric loss ($\tan\delta$) of the 75KNN-25SiO₂ and 80KNN-20SiO₂ glass ceramics with various heat treatment temperatures at 10 kHz to 1 MHz are illustrated. It can be seen that the dielectric constant increased with increasing heat treatment temperature. At higher heat treatment temperatures the dielectric constant and

loss are greatly increase, however these values decrease with an increase in frequency. Considering the SEM micrographs from Fig. 5.7 and the corresponding XRD patterns in Fig. 5.6, the higher of heat treatment temperature caused the larger size of KNN crystals leading to a higher value of dielectric constant. The variation in crystalline size distributions and also the distribution of KNN phase in the microstructure may cause the differences in the dielectric constant and loss values amongst the heat treated samples. The overall dielectric loss values of all glass ceramics were low, between 0.01 and 0.11 depending on the frequency. The maximum dielectric constant was found in the 80KNN-20SiO₂ glass-ceramic heat treated at 550°C, which is as high as 698 at 10 kHz with low value of $\tan\delta = 0.04$. This great increase in dielectric constant at high temperature of 80KNN-20SiO₂ may associate with the secondary phase and its crystalline size. Carefully investigation of these secondary phases should be performed in the future work.

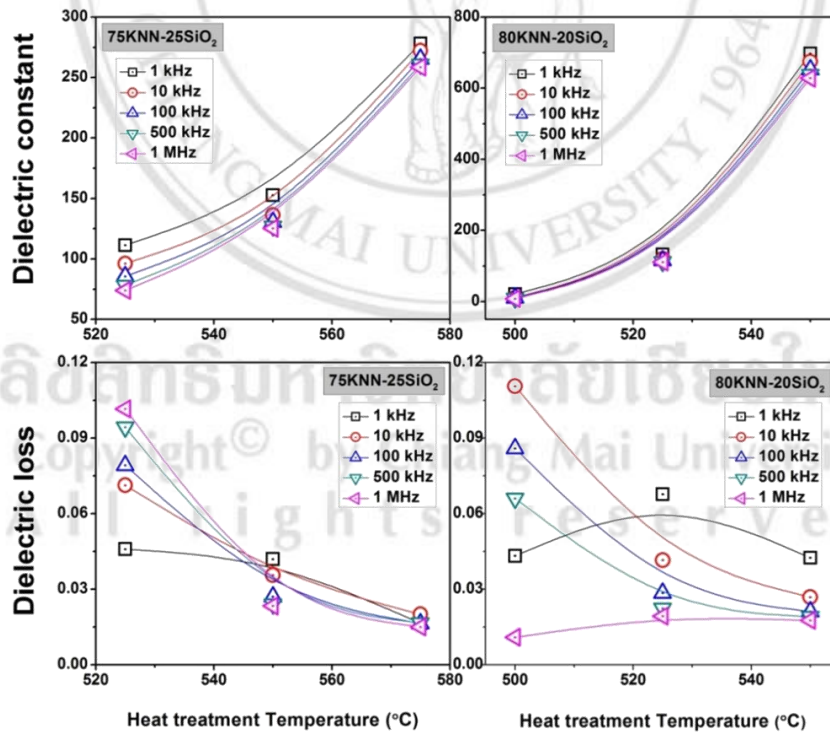


Figure 5.9 The dielectric constant and dielectric loss of 2 glass series heat treated at various temperature.

5.1.6 Optical properties

Fig. 5.10 – 5.11 shows the optical transmission spectra and Absorption in the UV - Vis - NIR region of the glass and glass ceramics 75KNN-25SiO₂ and 80KNN-20SiO₂ systems, respectively. The optical transmission spectra were all recorded at room temperature. The as-quenched samples are optically transparent. The transmittance of the heat-treated glass ceramics decreased greatly with increasing heat treatment temperature, while the absorption edges were found to shift toward higher wavelengths. The low transmittance of the glass-ceramic samples may be attributed to the light scattering due to the occurrence of crystals in the sample with sizes larger than 200 nm and hence the corresponding samples should be opaque. The refractive indices of these glass and glass ceramics lie between 1.64-1.66 which is higher than the typical silicate glass of (1.50), which may be due to the presence of the high permittivity KNN crystals. Considering the refractive index in Table 5.3 of the as-quenched glass and heat treated glasses which are approximately 1.65, these values shows that the light scattering at the crystal and glass matrix interface are not affected to the low transparency in glass ceramics. Fig. 5.12 showed the energy band gap of 2 glass series. It can be seen that the E_g were decreased with increasing heat treatment temperature.

Table 5.3 Refractive index of 75KNN-25SiO₂ and 80KNN-20SiO₂ glass systems.

Heat treatment temperature (°C)	Refractive index	E _g
75 KNN – 25 SiO₂		
As- quenched glass	1.65	4.07
525	1.655	3.68
550	1.655	2.89
575	1.64	1.98
80 KNN – 20 SiO₂		
As- quenched glass	1.65	4.06
500	1.66	3.68
525	1.66	-
550	1.65	-

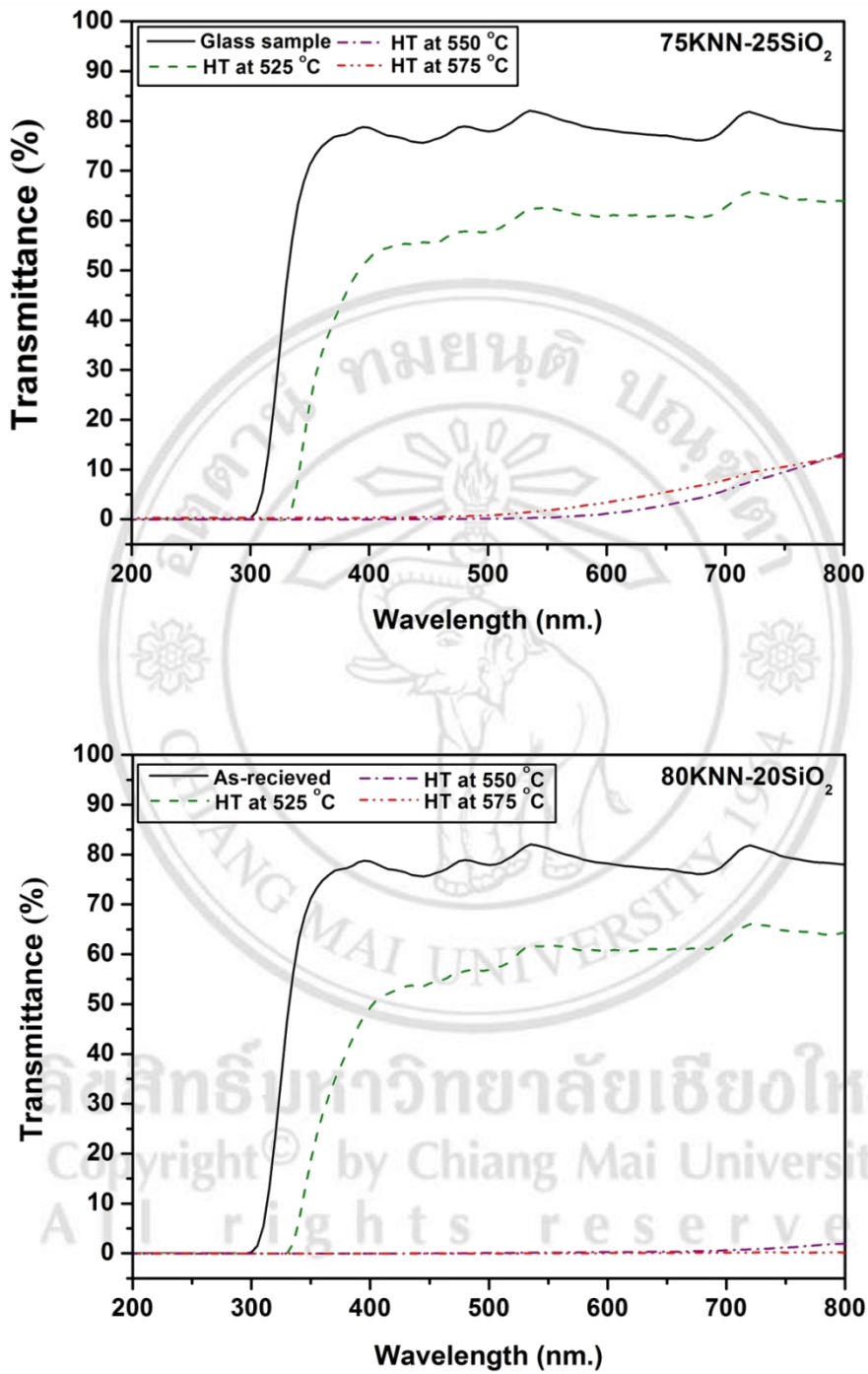


Figure 5.10 Percent transmittance of as-quenched glasses and glass-ceramic samples at various HT temperatures.

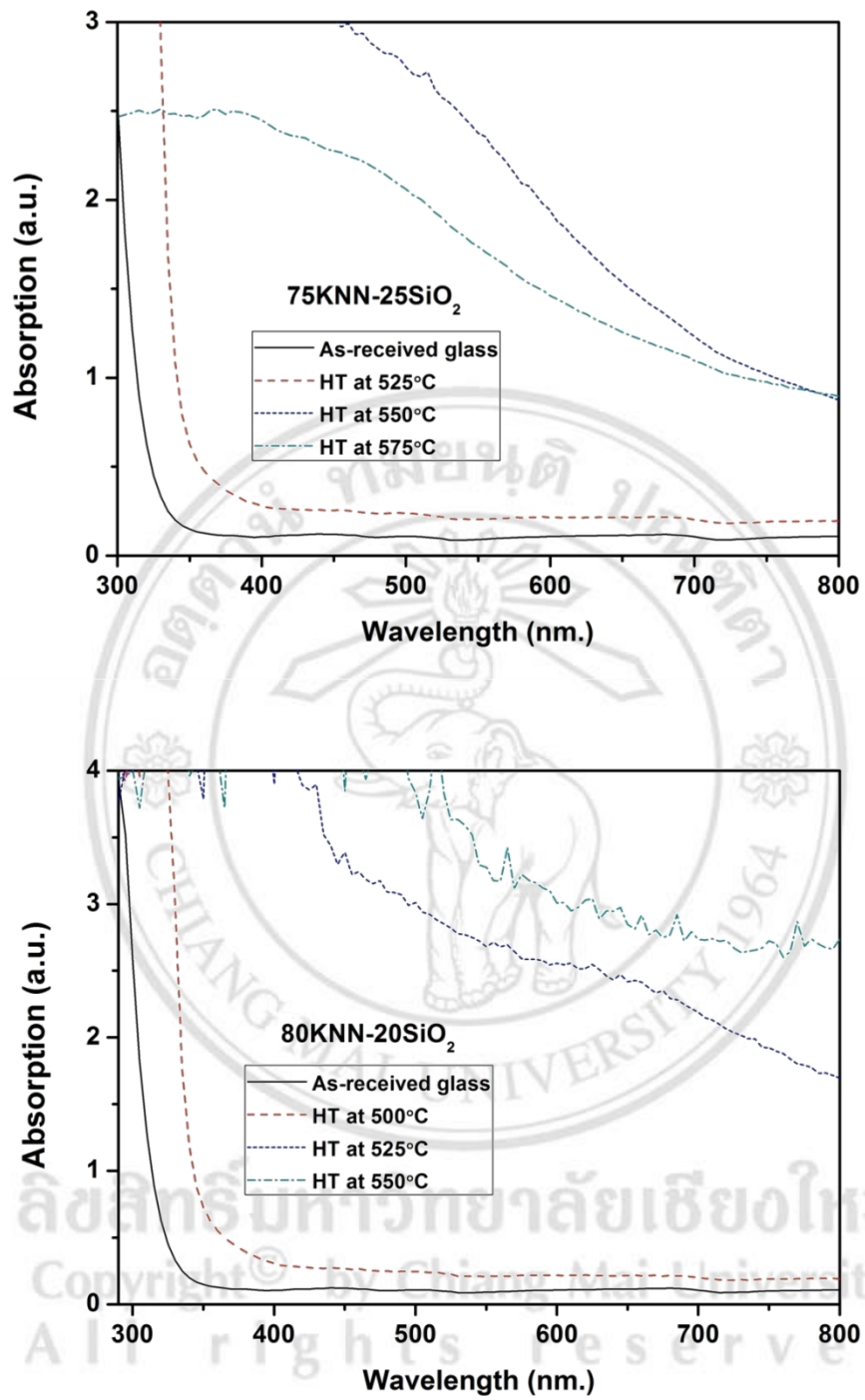


Figure 5.11 The absorption spectrum of as-quenched glasses and glass-ceramic samples at various HT temperatures.

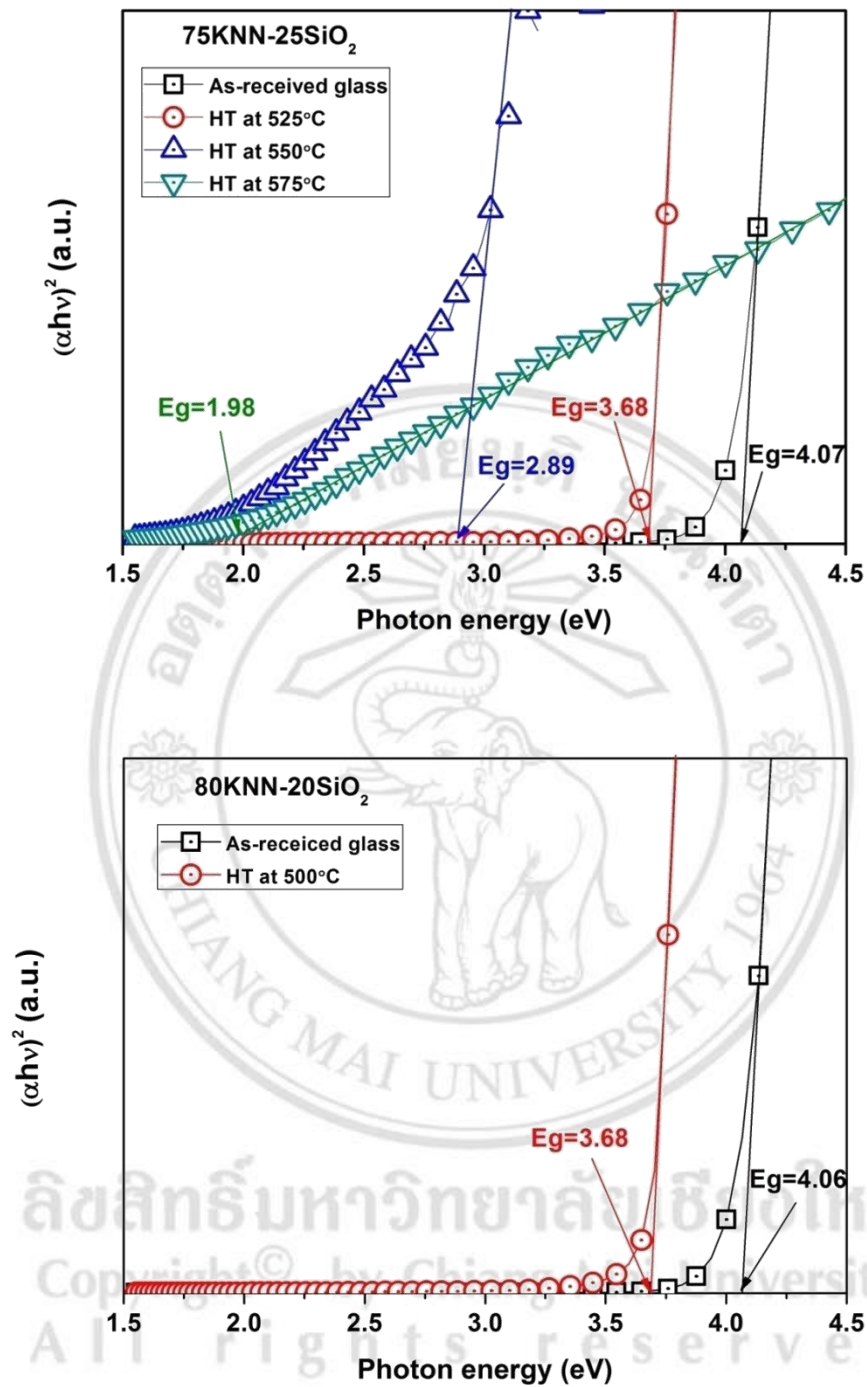


Figure 5.12 The energy band gap values of as-quenched glasses and glass-ceramic samples at various HT temperatures.

5.1.7 Conclusions

The fabrication of lead-free ferroelectric glass-ceramics from KNN based systems via incorporation method has been studied. It can be found that the heat treatment temperature plays a significant role in controlling the microstructure, crystallite sizes, and crystal quantity of the glass ceramics. Nano-crystals of KNN with lower crystallite size than 200 nm were precipitated in the silica glass matrix by lowest heat treatment temperature around 500°. The results on XRD, SEM, optical properties and dielectric properties confirm the formation of KNN nano-crystallite in the glass matrix using the incorporation technique. The crystallite sizes estimated from FESEM are in nanometer to micrometer scales depending on heat treatment temperature. The as-quenched glass is optically transparent with nearly 80% transmittance. The maximum dielectric constant found in 80KNN-20SiO₂ glass systems was 698 at 10 kHz with a low loss (tanδ) of 0.04 from the sample heat treated at 550°C, however, this sample also had the lowest transparency.

5.2 The characterization of Er₂O₃ doped KNN-SiO₂ glass and glass-ceramic

In this topic, the transparent glass-ceramics from Potassium Sodium Niobate (KNN)-silicate glass system doped with erbium oxide (Er₂O₃) were carried out by using incorporation method. In the incorporation method, a simple mixed-oxide technique was first employed to synthesize the KNN single phase powder before mixing with the glass former oxide and dopant of SiO₂ and Er₂O₃, respectively. KNN was added in glass batches as heterogeneous nucleating agent. The KNN powder was mixed with SiO₂ and Er₂O₃ dopant with KNN and Er₂O₃ content varied between 70-80 and 0.5-1.0 mol%, respectively. Each batch was subsequently melted at 1300°C for 15 minutes in a platinum crucible using an electric furnace. The quenched glasses were then subjected to heat treatment at various temperatures for 4 hours. The crystallization of the KNN crystals in the glass was accomplished by heat treatment processes which were also used to control the KNN crystal shape and size. Here, we report the thermal, electrical and optical properties of the prepared KNN glass-ceramics.

5.2.1 Thermal parameters

The DTA profile curve of Er₂O₃ doped KNN-SiO₂ glass and non-doped glasses (Fig. 5.12) provides thermal parameters, necessary for understanding the nature of resulting glasses and predicting the suitable temperatures for glass-ceramics samples. These DTA measurements were carried out in an air atmosphere at a heating rate of 5°C/min in the temperature range of 30°C - 800°C. The intense exothermic peak around 600°C is corresponding to crystallization (T_c). While, the noticeable endothermic peaks, representing by slight changes in slope of graphs as drawn by intersection point of two tangent lines at around 500°C, refer to the glass transition temperature (T_g). The 70KNN-30SiO₂ glass series has higher T_g than that found in 75KNN-25SiO₂ and 80KNN-20SiO₂, which may be resulted from the higher content of SiO₂ glass forming oxide. It can also be seen that the increasing of Er₂O₃ dopant increased the T_c in both glass systems as shown in Table 5.4.

The stability of glass can be estimated by those thermal parameters. The onset of T_c (or T_x) was applied to glass-forming criteria ($\Delta T = T_x - T_g$; Hruby's criterion [3]) for determining the ability of glass in forming nanostructured

glass-ceramics after applied energy from heat treatment process. The ΔT value of the 1.0 mol% Er_2O_3 doped glass was slightly increased comparing to that of the 0.5 mol% Er_2O_3 doped glasses as indicated in Table 5.4. From the ΔT value in Table 5.4, the stability of glass in composition of 70KNN-30SiO₂ with the higher SiO₂ content was higher than that of 80KNN-20SiO₂. Thus, the 80KNN-20SiO₂ glass is easy to devitrify which is not suitable for controlled crystallization in further glass-ceramic process.

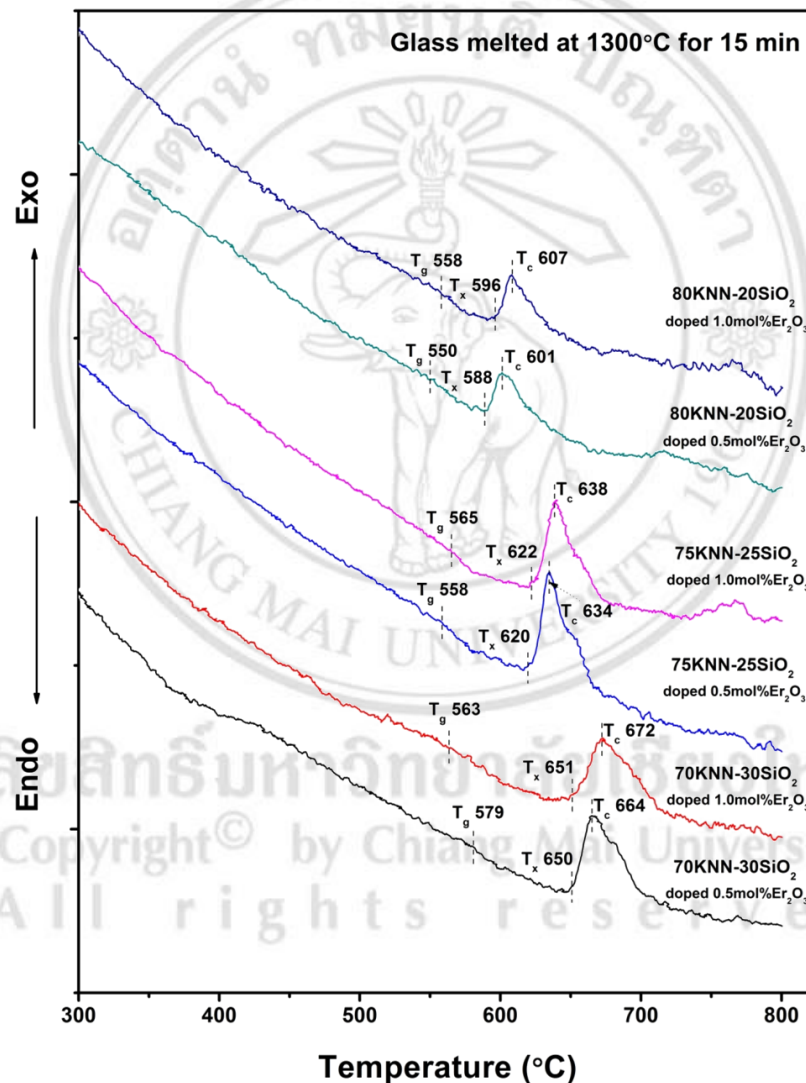


Figure 5.13 Thermal profile data of all glass samples by using DTA.

Table 5.4 The stability of glass-ceramics from their DTA thermal profile.

Glass conditions (mol%)	Er ₂ O ₃ (mol%)	T _g (°C)	T _c (°C)	T _x (°C)	ΔT (°C)
70KNN-30SiO ₂	0.5	579	664	650	38
	1.0	563	672	651	38
75KNN-25SiO ₂	0.5	558	634	620	62
	1.0	565	638	622	57
80KNN-20SiO ₂	0.5	550	601	588	88
	1.0	558	607	596	71

The heat treatment processes was employed at various temperatures depending on the observed thermal parameters from the DTA study in order to grow crystals inside the glass matrices. The appearances of the resulting glass-ceramics are shown in Fig. 5.13-5.15. It can be seen that glass-ceramics were all pink in color and the transparency of all glasses decreased with increasing heat treatment temperature.

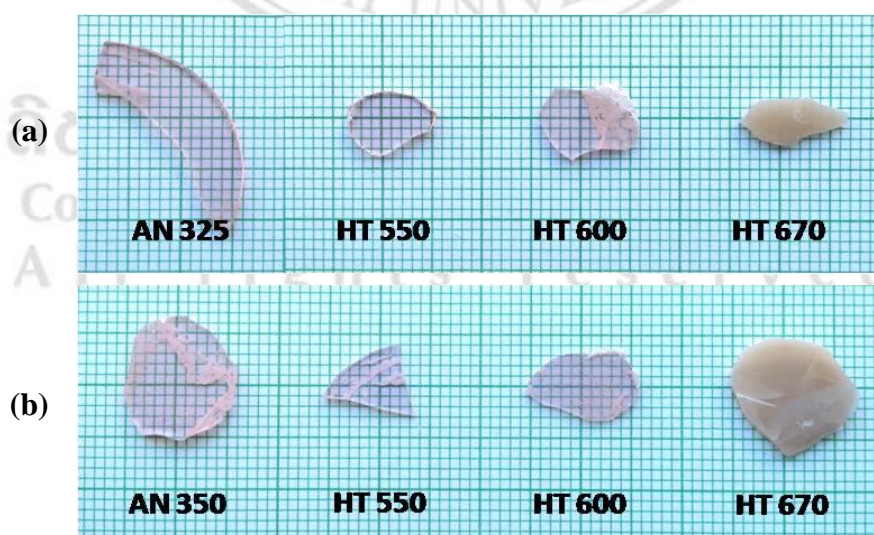


Figure 5.14 The appearance of glasses and glass-ceramics of 70KNN-30SiO₂ at various heat treatment temperatures. (a) doped 0.5mol% Er₂O₃, (b) doped 1.0mol% Er₂O₃.

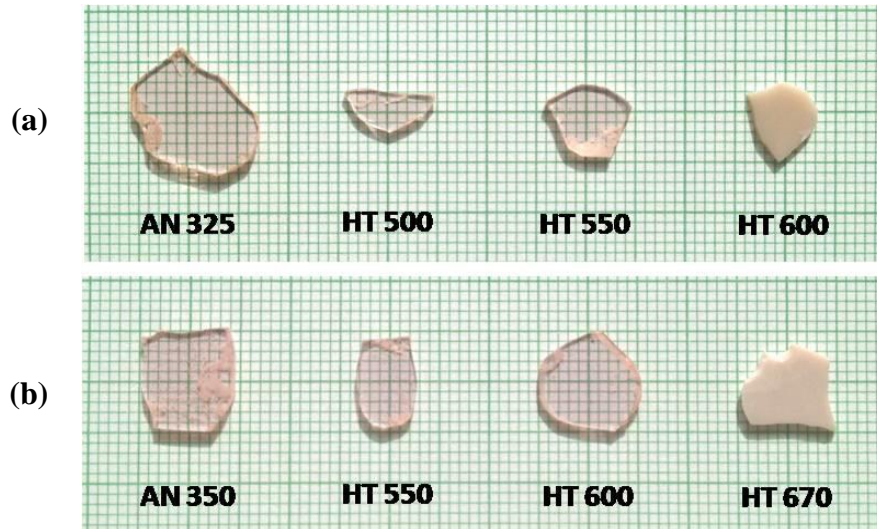


Figure 5.15 The appearance of glasses and glass-ceramics of 75KNN-25SiO₂ at various heat treatment temperatures. (a) doped 0.5mol% Er₂O₃, (b) doped 1.0mol% Er₂O₃.

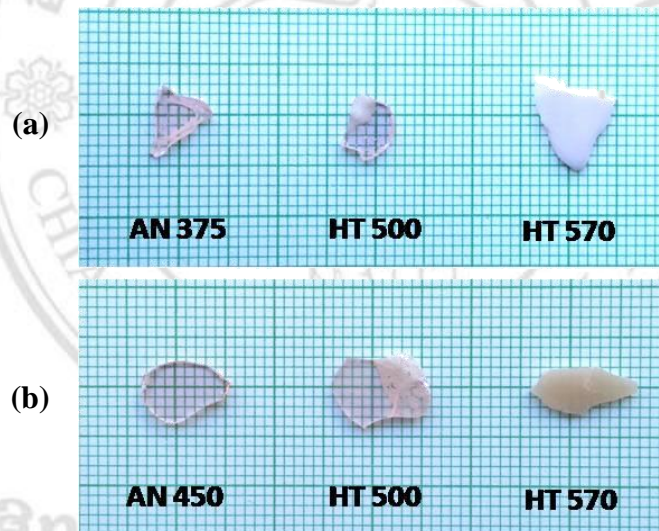


Figure 5.16 The appearance of glasses and glass-ceramics of 80KNN-20SiO₂ at various heat treatment temperatures. (a) doped 0.5mol% Er₂O₃, (b) doped 1.0mol% Er₂O₃

5.2.2 Densification investigation

The density of all glass and glass-ceramic compositions are showed in Fig. 5.16-5.18. The density of the 1.0mol% Er₂O₃ doped glass-ceramics is slightly higher that found in the 0.5mol% Er₂O₃ doped glass-ceramics. It can be noticed that the density of the glass-ceramics increases with increasing heat treatment temperature. This may correspond to the decrease in molar volume of the glass-ceramic sample during crystallization.

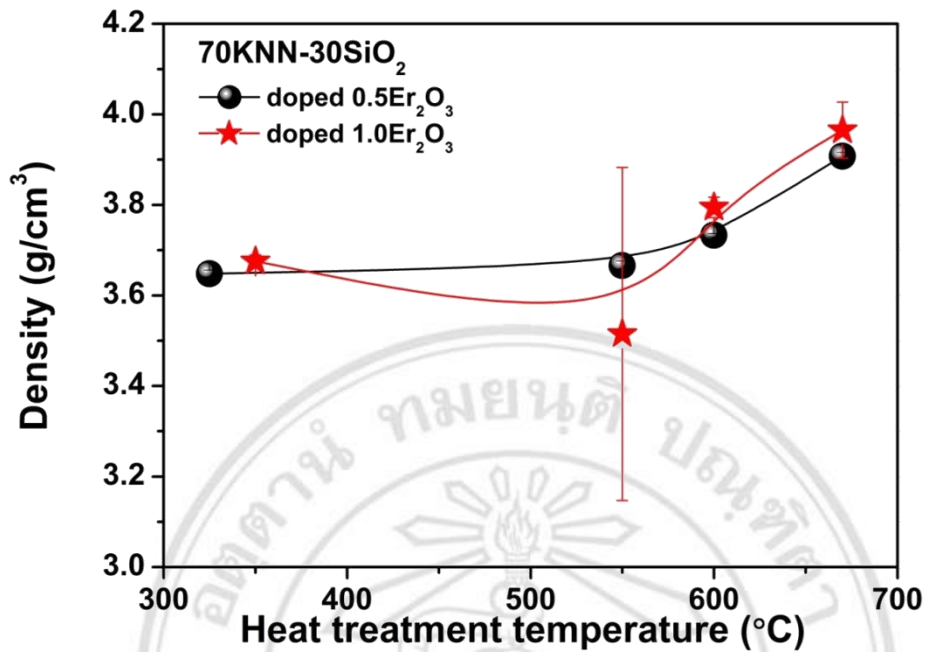


Figure 5.17 The density of glass ceramics 70KNN-30SiO₂ doped with 0.5 mol% and 1.0 mol% of Er₂O₃.

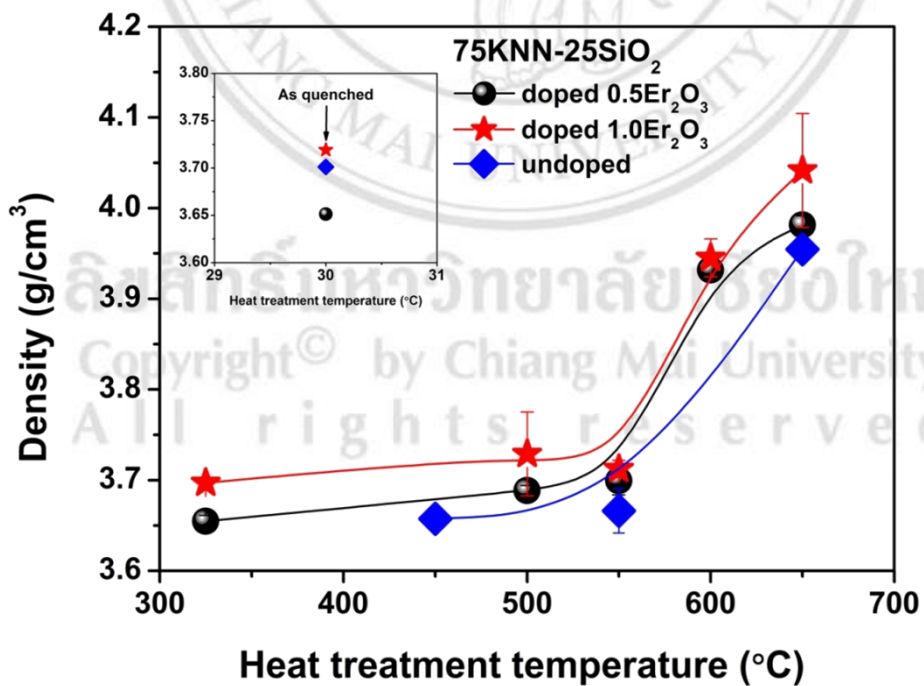


Figure 5.18 The density of glass ceramics 75KNN-25SiO₂ doped with 0.5 mol% and 1.0 mol% of Er₂O₃.

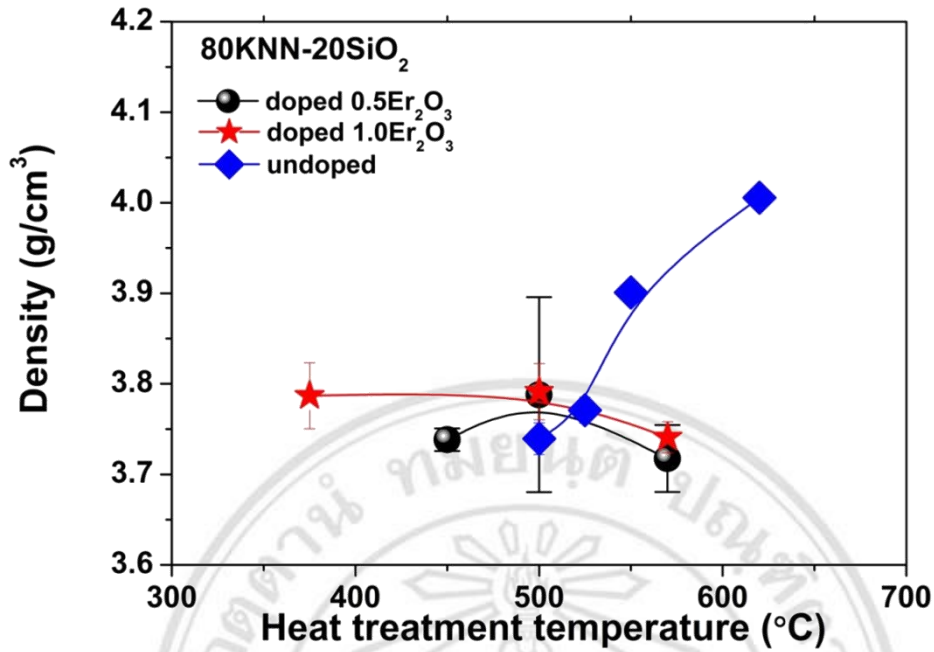


Figure 5.19 The density of glass ceramics 80KNN-20SiO₂ doped with 0.5 mol% and 1.0 mol% of Er₂O₃.

5.2.3 Structural formation

1) Phase composition studied by XRD

XRD diffraction patterns of the annealed glass and glass-ceramic samples as shown in Fig. 5.19 and 5.20. The amorphous nature has been found in the annealed 70KNN-30SiO₂ glasses of all doping conditions as indicated by their broad XRD peaks at around 30°, while those annealed 80KNN-20SiO₂ glass series contain noticeable XRD peaks, corresponding to K_{0.65}Na_{0.35}NbO₃ (KNN) phase (JCPDS 77-0038). This may be attributed to the lower ΔT value of the 80KNN-20SiO₂ glass series (Table 5.4), thus the KNN crystals has high tendency to devitrify during heat treatment process. After heat treatment, both 0.5 and 1.0 mol% Er₂O₃ doped 70KNN-30SiO₂ glasses still exhibits amorphous XRD patterns, until the heat treatment temperature rises up to 670°C which is near T_c of each glass, the KNN crystalline peaks starts to occur.

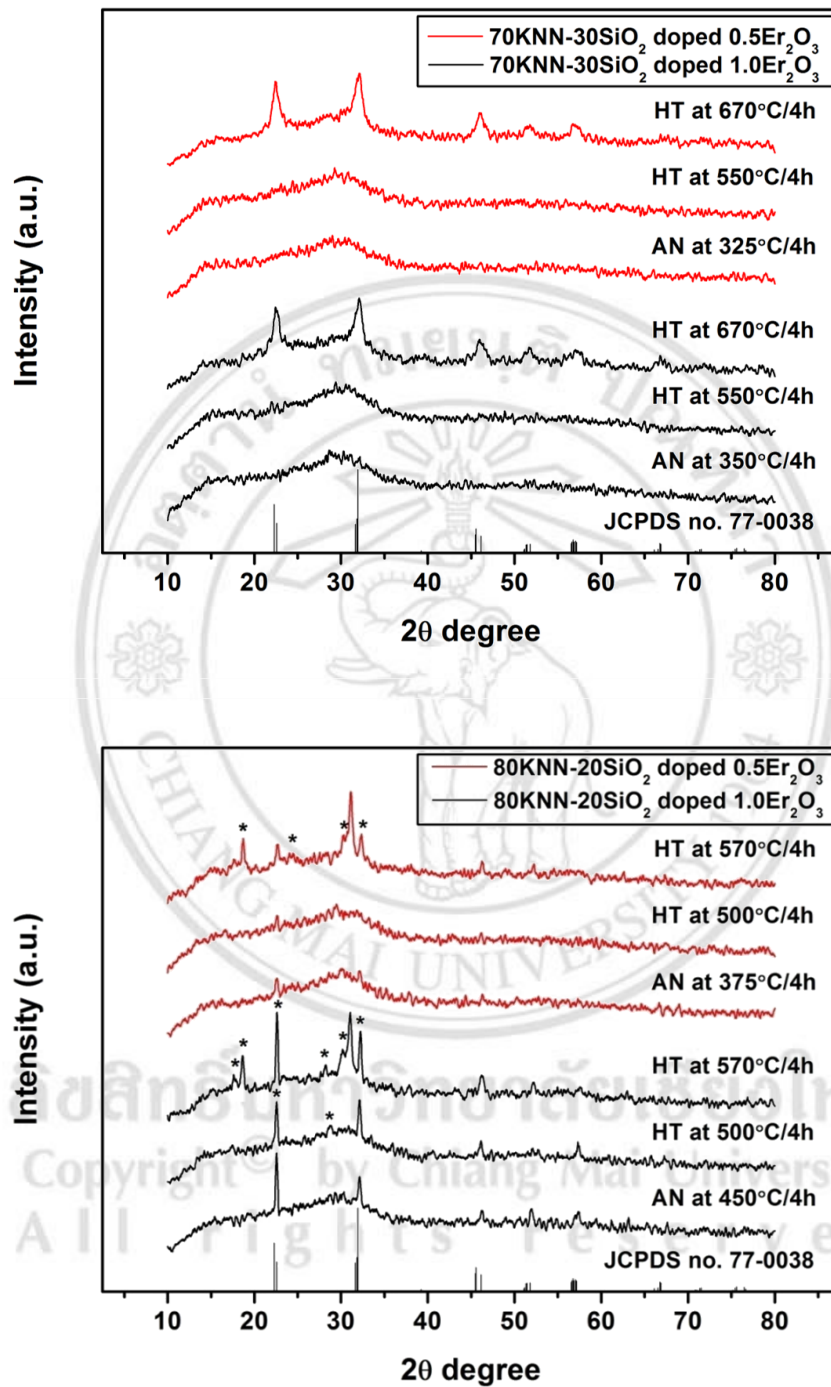


Figure 5.20 XRD pattern of 70KNN-30SiO₂ and 80KNN-20SiO₂ glass-ceramics doped 0.5-1.0mol% Er₂O₃ heat treated at various temperatures.

For 80KNN-20SiO₂ glasses, the KNN crystalline peaks appear in all samples, however the 1.0 mol% Er₂O₃ doped sample has higher degree of crystallinity than that of 0.5 mol% Er₂O₃ doped sample. The secondary phase (symbolized as *) is also observed in the samples heat treated at 570°C which is close to the T_c (~601-607°C) of each glass. The unusual behavior of the 80KNN-20SiO₂ glass-ceramic series should be corresponded to the low stability of glass as mentioned above. Many researches stated that the dopant of rare earth ions could occupied A site of perovskite structure as substitution defects with octahedral of oxygen coordination number of 12 and with a disorder neighbor shell, making strong emission of Er³⁺ [94-95,122]. Some of these mentioned that rare earth ions tend to precipitate and form cluster phase of Er³⁺. However, from our XRD pattern in Fig. 5.19, the erbium cluster was not existed because no diffraction peak of Er₂O₃ at about 29.05 (JCPDs no. 77-0464) was found, indicated that Er³⁺ had been incorporated well in KNN-SiO₂ host lattice. By the way, the peaks of KNN phases (at 47°, 52° and 57°) had a small shifted to the right because of Er³⁺ have been entered into KNN crystals, resulting in a slight distortion in crystal structure. These results suggest that Er³⁺ doped KNN structure exist between monoclinic to orthorhombic structure [130-131].

2) Phase formation studied by Raman

The raman spectra of KNN-SiO₂ doped 0-1mol% Er₂O₃ from Fig. 5.20 showed a different form from undoped conditions (topic 5.1.3). The glass-ceramics without Er₂O₃ exhibits 3 main scattering peaks at 246 cm⁻¹(ν₅), 604 cm⁻¹(ν₁) and 880 cm⁻¹(ν₁ + ν₅), which can be indicate typical perovskite structure of KNN. From Fig. 5.20, it can be seen that Er₂O₃ has huge effect to KNN silicate glass structure. In this work, Er₂O₃ doped KNN-SiO₂ show main peak around 520 and 830 cm⁻¹. The intense raman spectra at around 800 cm⁻¹ is relate to vibrations of less distorted NbO₆ octahedra or to NbO₆ octahedra sharing a corner with at least one other NbO₆ octahedra. Raman spectrum of 2 glass series corresponded to several structure. The band at 200–500 cm⁻¹ is

considered to be associated with Si-O-Si, a bending motion of SiO₄ [132]. While, The intense peak of about 850cm⁻¹ is relate to the vibration of NbO₆ distortion octahedral. However, the raman spectrum seem to be different after heat up to T_c. At T_c point, glass-ceramics are clearly showed raman shift peak of silica at 440cm⁻¹ and 550cm⁻¹, which is related to bending mode and stretching mode, respectively. However, the broad peak around 650-900cm⁻¹, in which corresponded to Nb-O octrahedral still showed up.

5.2.4 Microstructural observation

SEM micrographs of the glass ceramics are shown in Fig. 5.21 and 5.22. These micrographs show a bulk crystallization of the KNN phase with a different shapes observed for the glass matrices of all heat-treated samples. At 550°C and 500°C in glass composition of 70KNN-30SiO₂ (Fig. 5.21) and 80KNN-20SiO₂ (Fig. 5.22), the small bulk of KNN was observed and the crystal showed a rectangular in shape. Then at highest heat treatment temperature, crystals changed to irregular shape. It can be seen that all of the glass-ceramics have crystal size lower than 1 μm. but still too large (>200 nm.) to be transparent, giving rise to opaque bulk glass-ceramics. This is consistent with the XRD result. The crystallinity of the solid solution of (K,Na)NbO₃ crystals increased with increasing HT temperature. The highest degree of crystallinity was found in the glass-ceramic sample heat treated at T_c.

ลิขสิทธิ์มหาวิทยาลัยเชียงใหม่
Copyright © by Chiang Mai University
All rights reserved

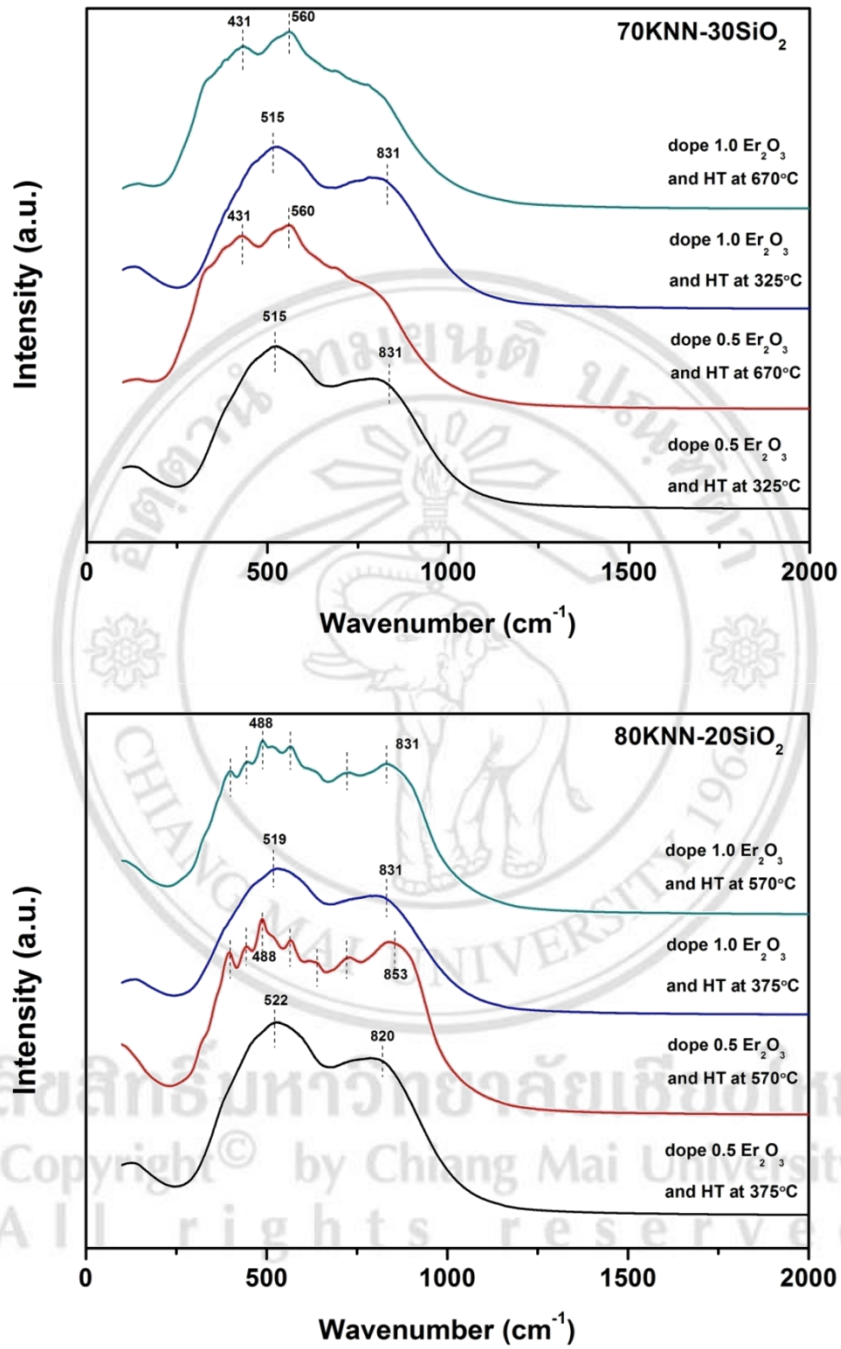


Figure 5.21 The raman spectra of 70KNN-30SiO₂ and 80KNN-20SiO₂ doped 0.5 and 1.0 mol% Er₂O₃ and heat treated at T_g and T_c, respectively.

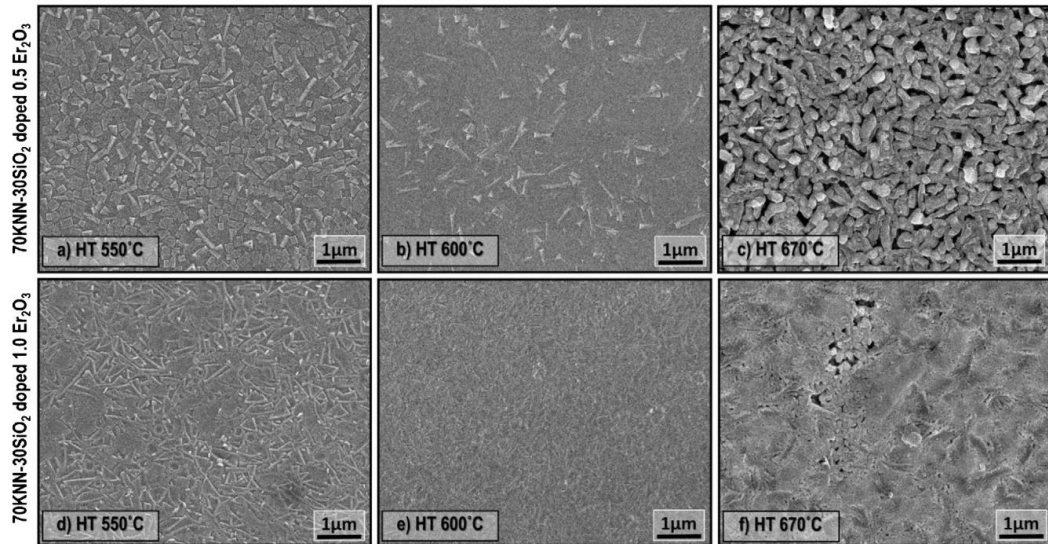


Figure 5.22 SEM micrographs of glass-ceramics 70KNN–30SiO₂ doped 0.5–1.0 Er₂O₃ heat treatment at 550°C (a, d), 600°C (b, e) and 650°C (c, f).

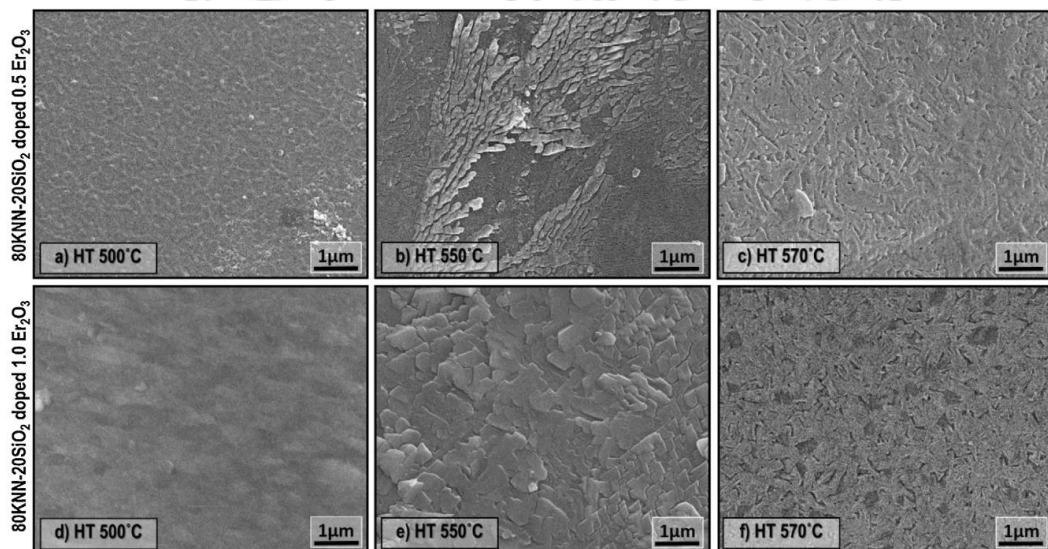


Figure 5.23 SEM micrographs of glass-ceramics 80KNN–20SiO₂ doped 0.5–1.0 Er₂O₃ heat treatment at 500°C (a, d), 550°C (b, e) and 570°C (c, f).

5.2.5 Electrical property

Fig. 5.23 shows the dielectric constants and their dielectric loss of the 70KNN-30SiO₂ and 80KNN-20SiO₂ glass and glass-ceramics doped with 0.5mol% and 1.0mol% of Er₂O₃ at various heat treatment temperatures. It can be found that the dielectric constant of the glass-ceramics at lower heat treatment temperature of less than 600°C lies between 120-150. This may be due to the lower crystallinity of the KNN phase in these samples as described in the XRD result. This can be confirmed that the higher dielectric constant of about 458.41 and 417.36 at 100 kHz were found in the high crystallinity of 0.5 and 1.0 mol% Er₂O₃ doped 70KNN-30SiO₂ glass-ceramic samples, respectively, both heat treated at 670°C.

Considering the work done by R.S. Chaliha [95], their glass-ceramics containing potassium niobate (KNbO₃) crystals doped with Er³⁺ ions showed the average dielectric constant (ϵ_r) at about 17, which was higher than sodium silicate glasses ($\epsilon_r = 7 - 10$) and borosilicate glasses ($\epsilon_r = 4.5 - 8$). This might become from the ionic size of Nb⁵⁺ are too high. Chaliha's report also showed that heat treatment time was significant to dielectric constant due to the possibility to increase crystal size of KNbO₃. Thus, the higher dielectric constant in this work are attributed to the high dielectric constant KNN phase which is the solid-solution of KNbO₃. Moreover, the overall dielectric loss (tan δ) of the KNN-SiO₂ glass-ceramics is in a low range of 0.001-0.007 depending on each composition, except that of the 1.0 mol% Er₂O₃ doped 80KNN-20SiO₂ glass-ceramic samples. This may be useful in the applications in capacitors and microwave devices.

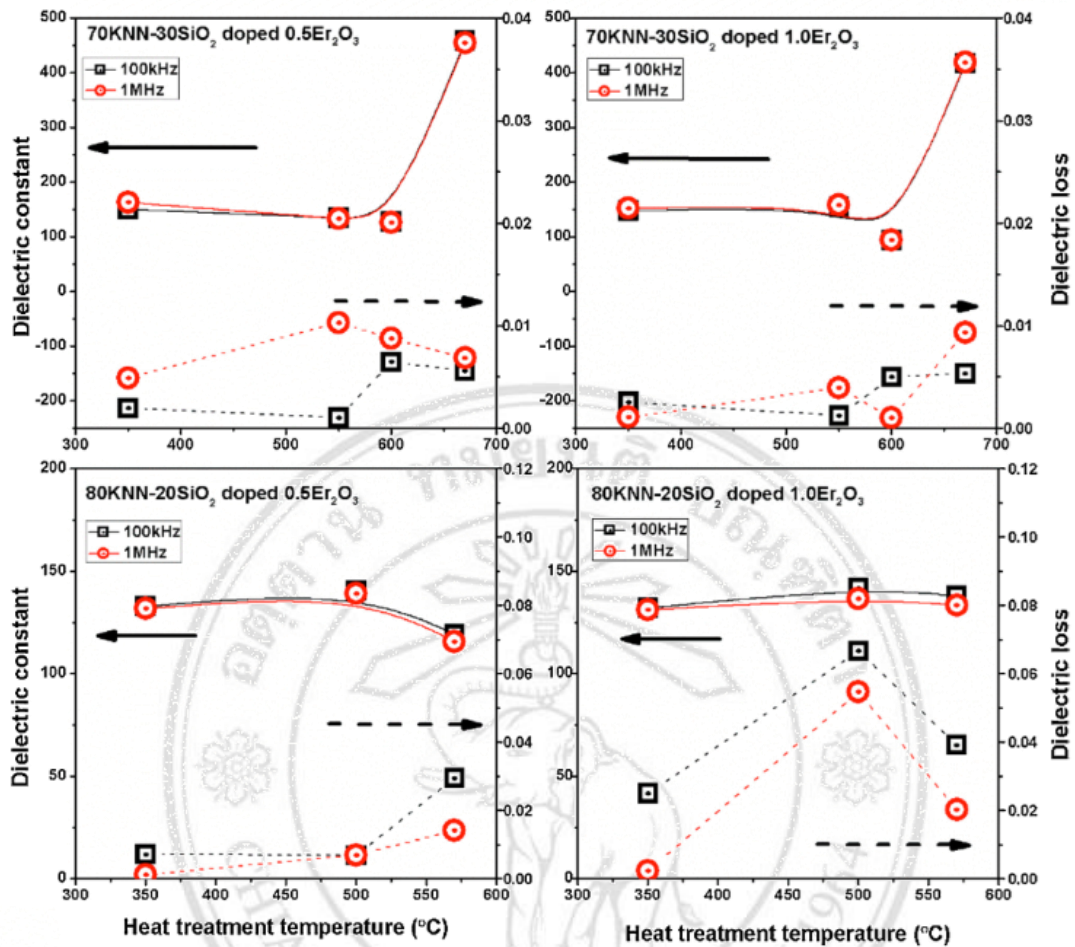


Figure 5.24 Dielectric constant and dielectric loss of 2 glass-ceramic conditions after various heat treatment temperatures.

5.2.6 Optical property

1) Absorbance

UV-Vis absorption spectra (Abs%) of the prepared glasses and glass-ceramics are shown in Fig. 5.24. It can be seen that Abs% is increased with increasing heat treatment temperatures. The effect of heat treatment temperature on the transparency of glass originates from the type and size of crystals precipitated in the glass matrix. For visible light, samples containing crystals larger than 200 nm cause light scattering and hence the respective samples should be opaque. Transparent samples should contain crystals lower than 200 nm and also a small crystal size distribution [13]. From Fig. 5.24, all of the absorption peaks are f-f transition of Er^{3+} ions reported by Carnall's

conversion [133] as $^4I_{15/2} \rightarrow ^2G_{9/2}$ (365 nm), $^4G_{11/2}$ (377 nm), $^2H_{9/2}$ (406 nm), $^4F_{5/2} + ^4F_{3/2}$ (450 nm), $^4F_{7/2}$ (488 nm), $^2H_{11/2}$ (521 nm), $^4S_{3/2}$ (544 nm), $^4F_{9/2}$ (651 nm), $^4I_{9/2}$ (799 nm) and $^4I_{11/2}$ (978 nm). Glass-ceramics display strong absorption edges below 350 nm. These absorption edges around 300 nm are transparent in all visible regions except intrinsic absorption lines due to Er^{3+} ions dopant [134]. However, the absorption edge at around 400 nm corresponded to nonlinear absorption via a two photon process which is an important mechanism of down-converting energy process. These results are similar to that of previous works, studied in silicate and tellurite glasses [135-136]. This indicates that the laser active Er^{3+} ions have entered into the $(K,Na)NbO_3$ crystalline phase. Similar results were reported recently [95,137]. The optical band gap was obtained by plotting $(\alpha h\nu)^2$ versus $h\nu$ (where α is the absorption coefficient and $h\nu$ is the photon energy) as shown in Fig. 5.25, 5.26 and 5.27, which is described by equation 4.3 [138-139].

The optical band gap, E_g of the selected transparent glass-ceramics was found to vary between 2.85 and 3.75 eV as tabulated in Table 5.5. It can also be noticed that the increase amount of Er_2O_3 dopant from 0.5 to 1.0 mol% has shown insignificant effect on modifying energy band gap of each glass series.

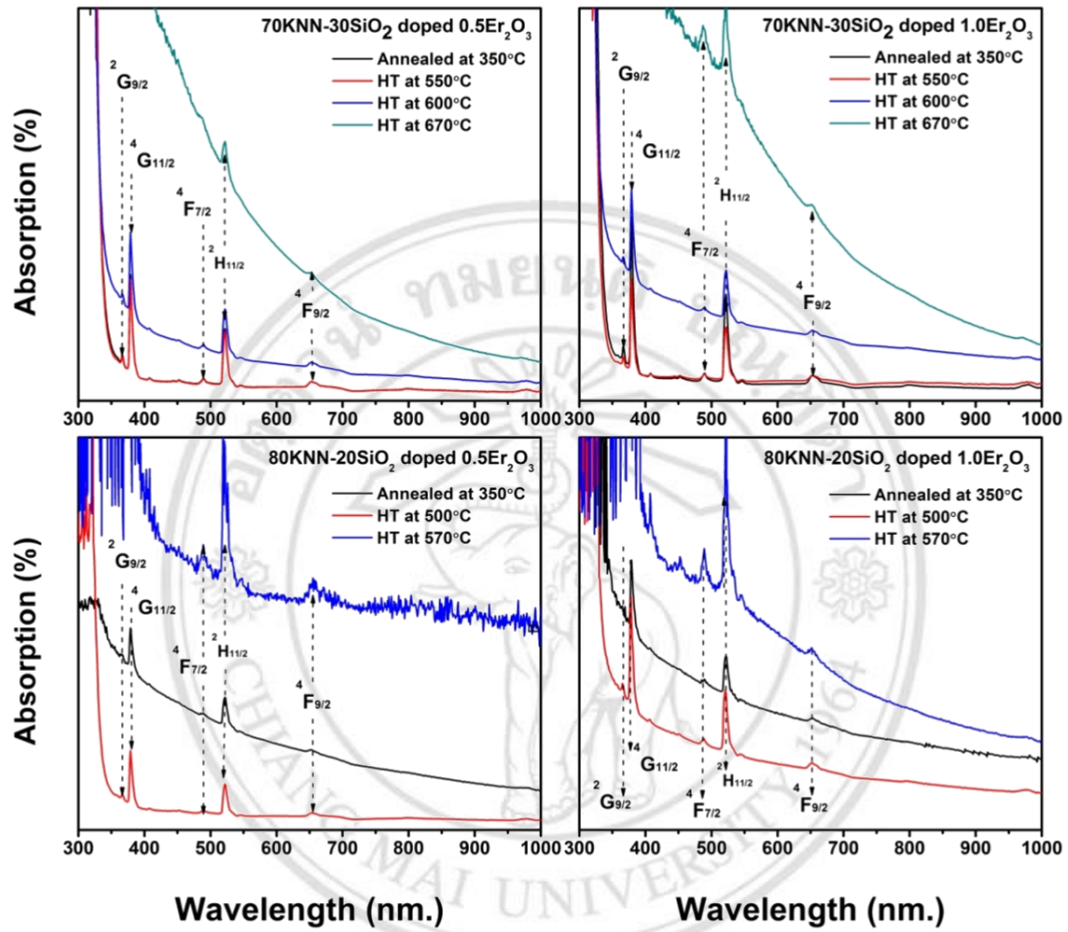


Figure 5.25 Absorption spectra of the Er³⁺ doped KNN-SiO₂ glass-ceramics heat treated at various temperatures.

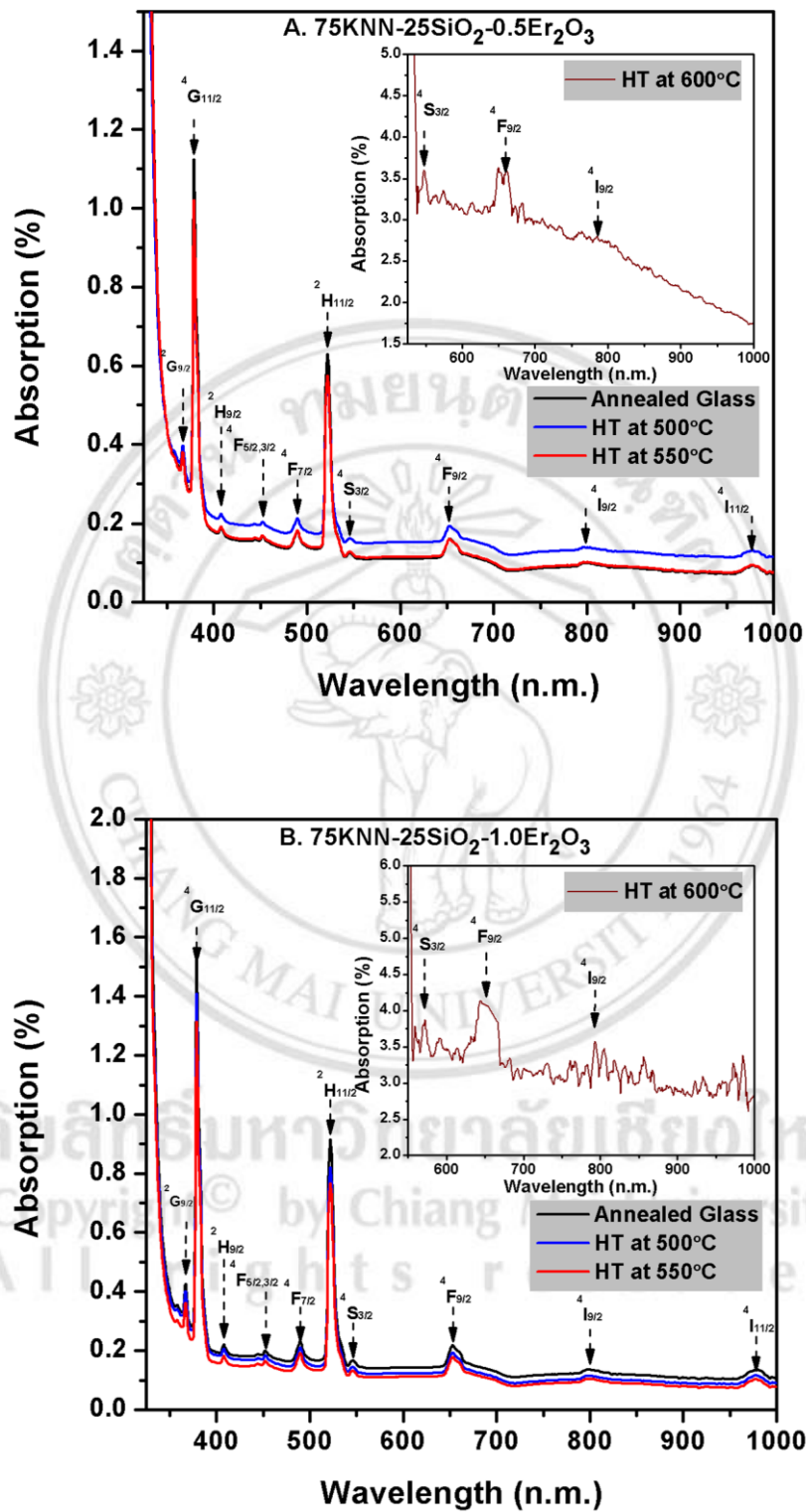


Figure 5.25 (continue) Absorption spectra of the Er³⁺ doped KNN-SiO₂ glass-ceramics heat treated at various temperatures.

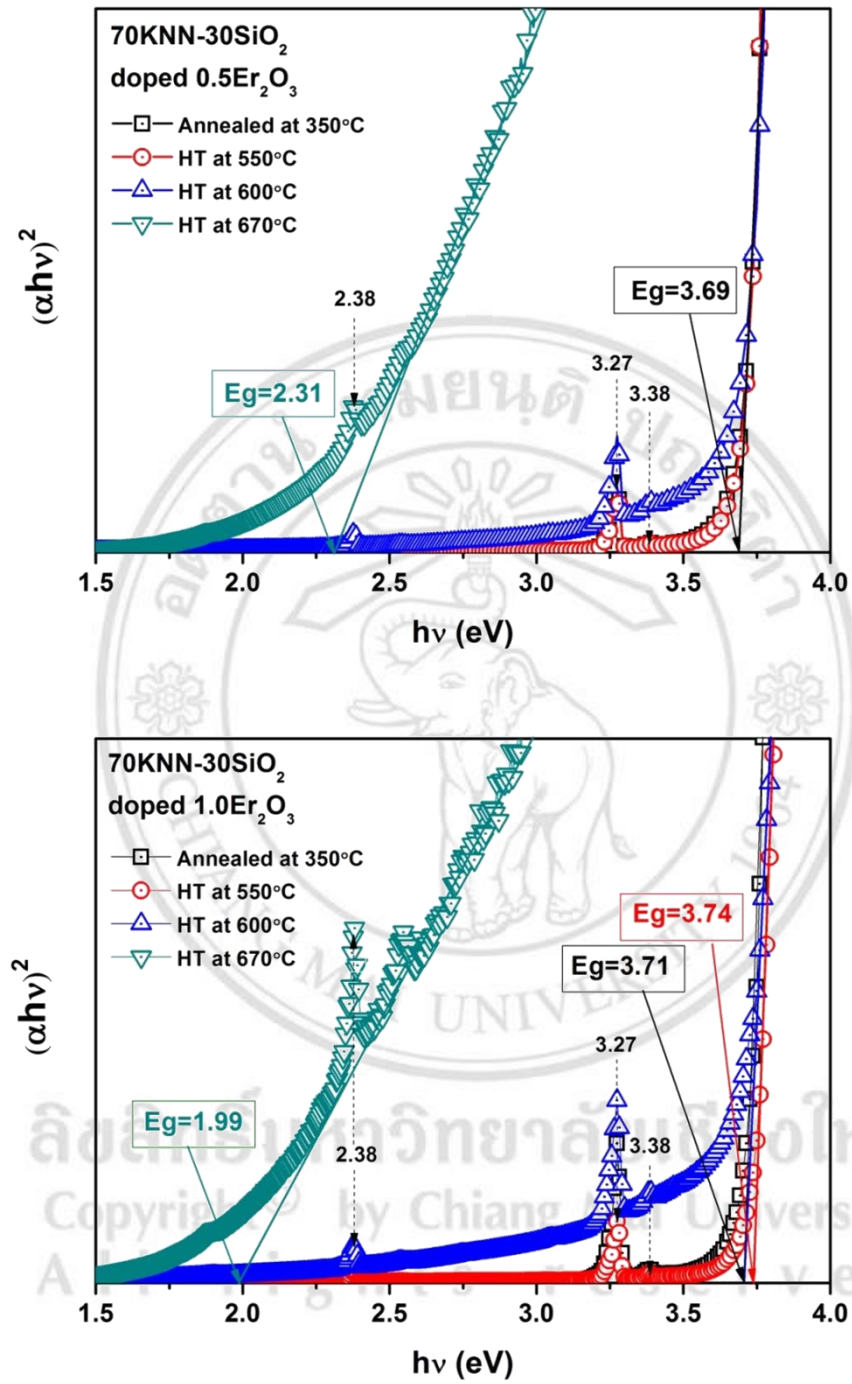


Figure 5.26 Plots of $(\alpha h\nu)^2$ versus $h\nu$ of the Er³⁺ doped 70KNN-30SiO₂ glass-ceramics.

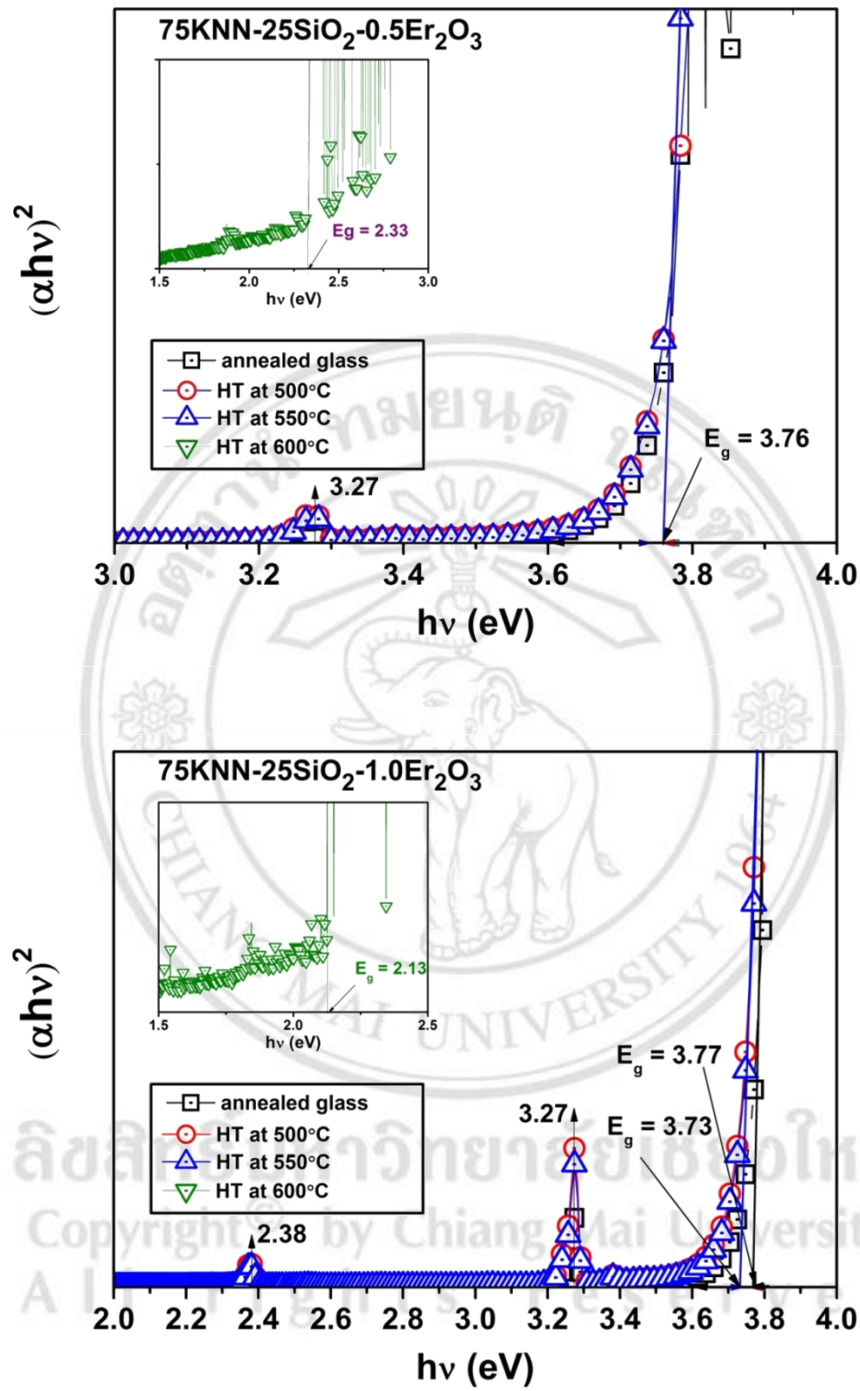


Figure 5.27 Plots of $(\alpha h\nu)^2$ versus $h\nu$ of the Er³⁺ doped 75KNN-25SiO₂ glass-ceramic.

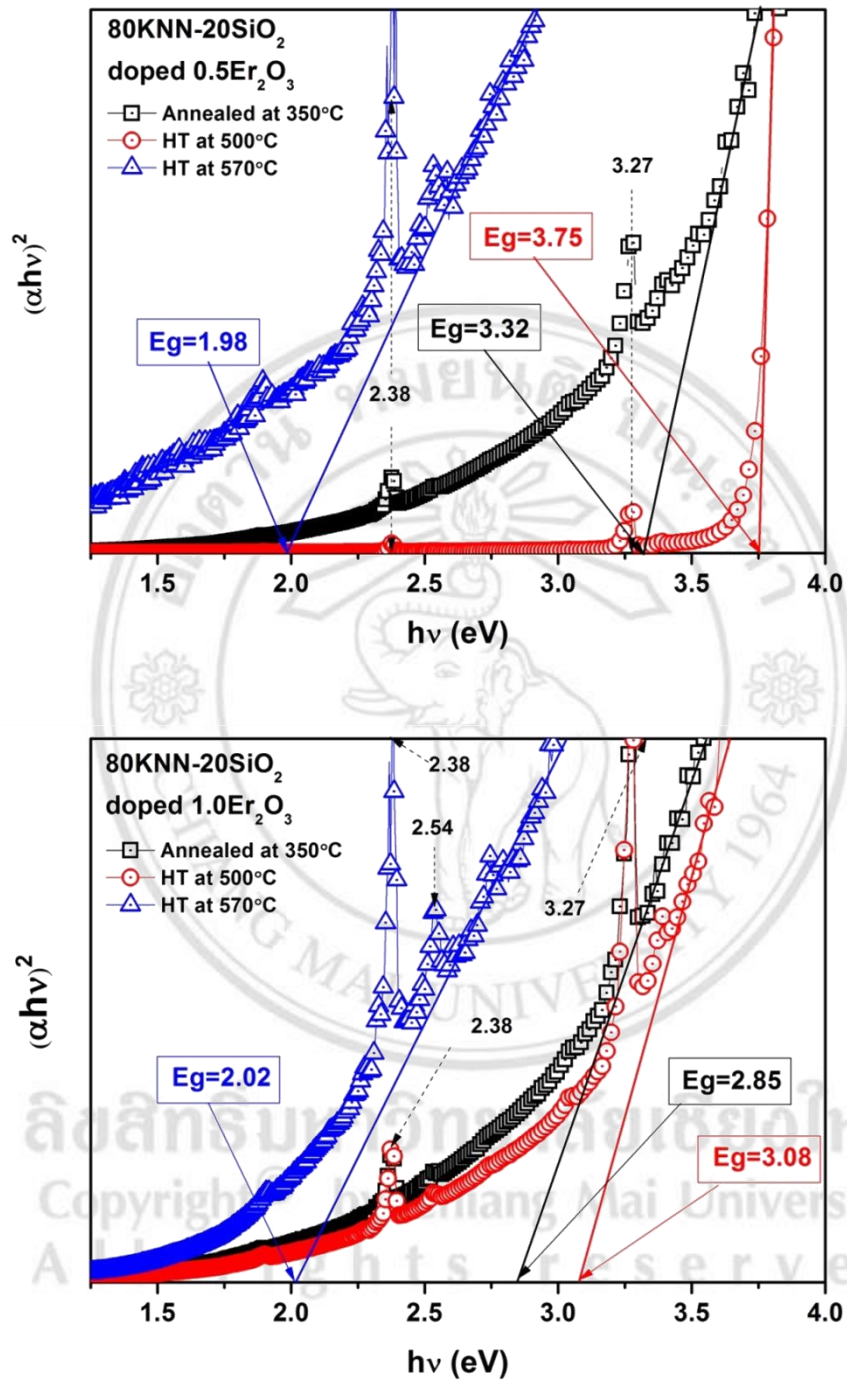


Figure 5.28 Plots of $(\alpha h\nu)^2$ versus $h\nu$ of the Er^{3+} doped 80KNN-20SiO₂ glass-ceramics.

Table 5.5 Calculated energy band gap (E_g) of the Er^{3+} doped KNN- SiO_2 glass-ceramics heat treated at various temperatures.

Glass condition (mol%)	Er_2O_3 content (mol%)	Treatment temperature ($^{\circ}C$)	E_g (eV)
70KNN-30 SiO_2	0.5	350	3.69
		550	3.69
		600	3.69
		670	2.31
	1.0	350	3.71
		550	3.74
		600	3.74
		670	1.99
80KNN-20 SiO_2	0.5	350	3.32
		500	3.75
		570	1.98
	1.0	350	2.85
		500	3.08
		570	2.02

2) Photoluminescence spectra

In Fig. 5.28, showed the visible emission of Er_2O_3 doped 75KNN-25 SiO_2 glass and the effect of heat treatment temperature to glass ceramics. All of glass ceramics emit bright green light under 315-410 nm excitation. This ultraviolet excitation in range 315-410 nm also activated the electrons at the $^4I_{15/2}$ to $^4G_{11/2}$ and $^4G_{9/2}$ states of Er^{3+} ion co-doped materials. The fluorescence at 515-542 nm and 542-577 nm as shown in Fig. 5.29 are green luminescence correspond to the $^2H_{11/2} \rightarrow ^4I_{15/2}$ and $^4S_{3/2} \rightarrow ^4I_{15/2}$ transition respectively. The energy level diagram of Er^{3+} was shown in Fig. 5.30. This wide range of ultraviolet excitation brought to energy conversion to lower state with 2 mechanisms. First, after excitation to $^4G_{11/2}$ and $^4G_{9/2}$ levels, there is a fast non-radiative decay to $^2H_{9/2}$ level follow by a radiative decay to the $^4I_{15/2}$ and $^4I_{13/2}$ with emission at 410 nm and 556nm, respectively. Second, a non-radiative decay to $^4S_{3/2} - ^2H_{11/2}$ levels follow by radiative decay to the ground level yields photon at 520 and 545 nm, respectively.

It can be seen from the Fig. 5.28 that the fluorescence intensity of higher heat treatment sample was decreased, due to the increase of crystallization as confirmed by SEM micrograph. Normally, the shifting in the peak positions of emission spectra and the decrease of the FWHM value of glass-ceramics indicated that the rare earth ions entered to glass-ceramics structure but in a less amount into the crystalline phase thus formed. Thus, even though heat treated sample at 600°C showed very low emit green light but no obvious shifting of the peaks was observed, means the crystal field around the erbium ions in all samples had not been change during heating in the samples.

The intense fluorescent of glass-ceramics is corresponded to the incorporation of rare earth ions in a non-centrosymmetric host. Generally, in the perovskite-structure like (K,Na)NbO₃ crystals, K⁺, Na⁺ and Nb⁵⁺ occupy octahedral sites with C₃ or nearly C_{3v} point symmetry. In alkaline silicate glasses, NbO₆ octahedral was main framework and display as lattice former in the Si-O bonds containing SiO₄ tetrahedral network. The Na⁺ and K⁺ ions have the same occupancy factor of 0.5 and share eight distinct crystal sites.

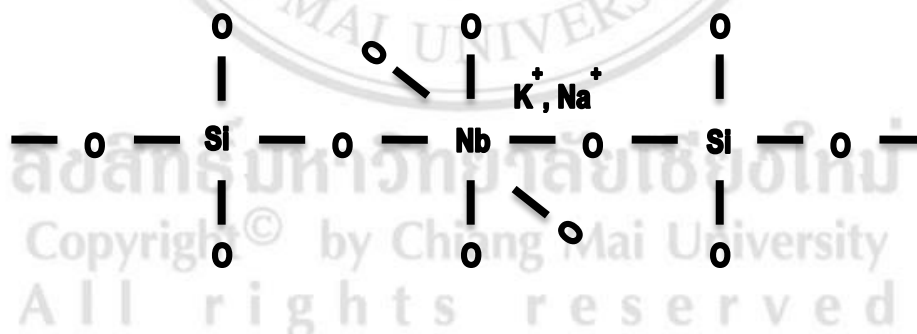


Figure 5.29 Schematic of glass-ceramics composition [137].

When the rare earth ion is entering in the crystal, it prefers to replace A⁺ site forming [REO₆]⁹⁻ octahedron [137]. Hence, In this work, Er³⁺ ions are possible partial replaced A⁺ ion site (K⁺ and Na⁺) in KNN structure because of their ionic radius aren't different (Er³⁺=1.04Å, Na⁺= 1.18Å and K⁺=1.33Å). Normally, the replacement of exceed charge carrier with host ion lead to grasp the oxygen bond making

distortion in the lattice structure [95], which confirmed the XRD result as mention above.

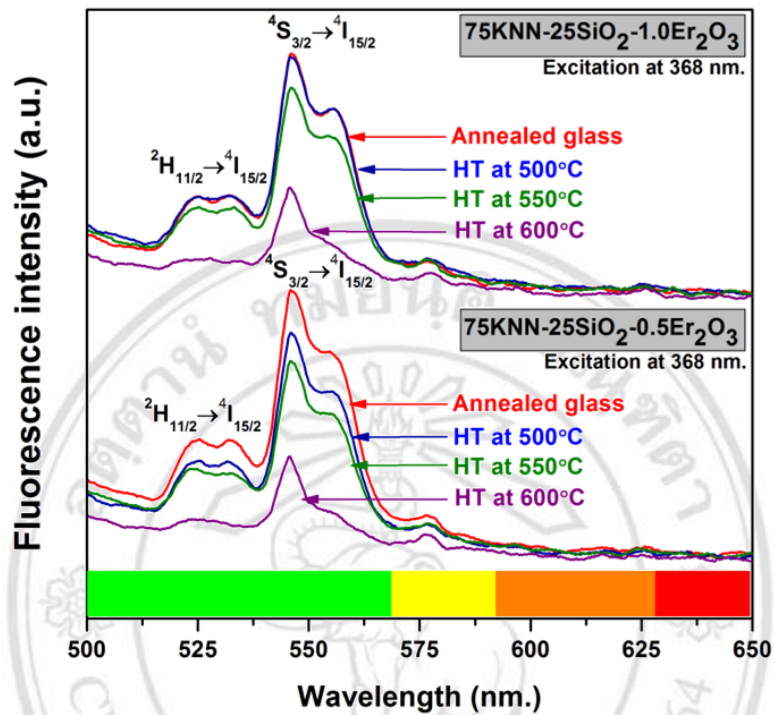


Figure 5.30 Photoluminescence spectra of 75KNN-25SiO₂ doped 0.5mol% Er₂O₃ and 1.0mol% Er₂O₃ under 310-415 nm excitation.

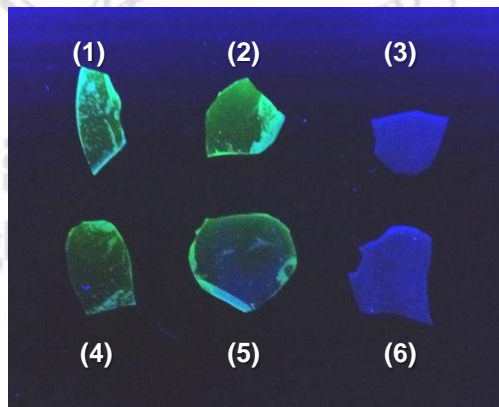


Figure 5.31 Photograph of glass ceramics 75KNN-25SiO₂ doped 0.5mol% Er₂O₃, (1) HT500, (2) HT550, (3) HT600, and 1.0mol% Er₂O₃ (4) HT500, (5) HT550 (6) HT600 luminescence under 310-415 nm excitation (HT= heat treatment temperature).

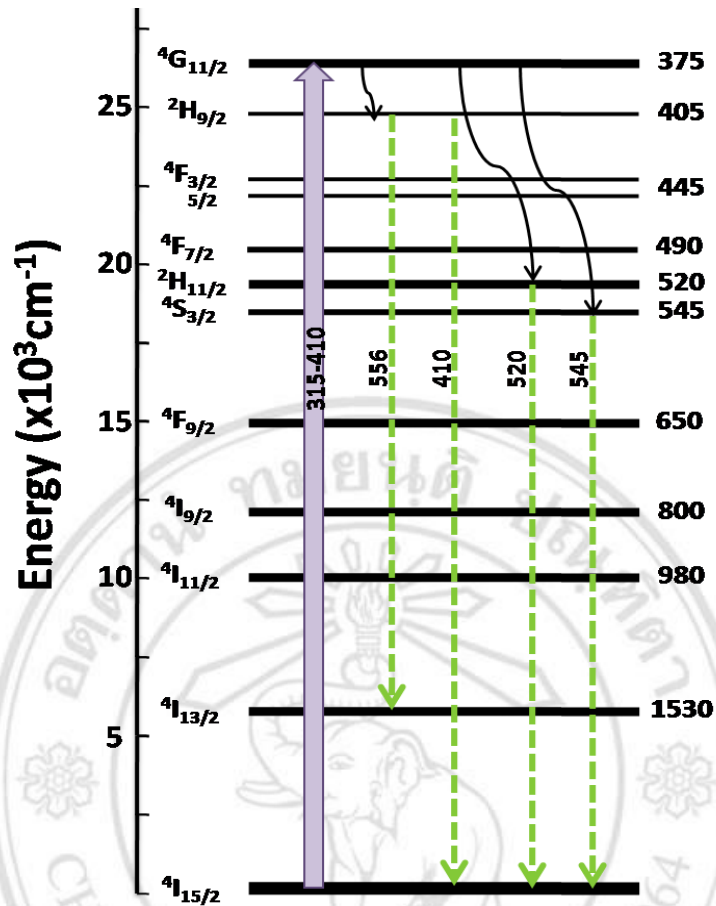


Figure 5.32 Energy level diagram of Er^{3+} ions with luminescence mechanism.

5.2.7 Conclusions

In this research, transparent KNN- SiO_2 glass-ceramics doped Er_2O_3 have been successfully prepared by incorporation method. It was indicated that heat treatment temperature plays a significant role in controlling the microstructure, crystallite sizes, and crystal quantity of the glass ceramics. The maximum dielectric constant of about 458.41 at 100 kHz with a low $\tan\delta$ of 0.005 could be obtained from the glass-ceramic sample of 70KNN-30 SiO_2 doped 0.5mol% Er_2O_3 and heat treated at 670°C . From optical study, the transparency value dropped with an increase in the heat treatment temperature. It can be seen that the small amount of rare earth Er_2O_3 oxide plays an insignificant role in improving the energy state by increasing energy band gap in the KNN- SiO_2 glass-ceramics.